INHIBITION OF THE BACTERIAL SIALIC ACID SYNTHASE, NEUB

INHIBITION OF THE BACTERIAL SIALIC ACID SYNTHASE, NEUB

By

VLADIMIR POPOVIĆ, B. Sc.

A Thesis

Submitted to the School of Graduate Studies

In Partial Fulfillment of the Requirements

For the Degree

Master of Science

McMaster University

MASTER OF SCIENCE (2012) McMaster University

(Chemical Biology Graduate Program) Hamilton, Ontario

TITLE: Inhibition of the bacterial sialic acid synthase, NeuB

AUTHOR: Vladimir Popović, B. Sc. (Brock University)

SUPERVISOR: Dr. Paul J. Berti

NUMBER OF PAGES: xi, 62

Abstract

Sialic acid synthase (NeuB) is a key enzyme in bacterial biosynthesis of the sialic acid *N*-acetylneuraminic acid (NeuNAc). It catalyzes the addition of phosphoenolpyruvate (PEP) to *N*-acetylmannosamine (ManNAc) in the presence of a divalent cation such as Mn^{2+}. We have explored the inhibition of NeuB by an oxacarbenium ion mimic, NeuNAc oxime, and hydroxylamine (NH_2OH). NeuNAc oxime shows slow-binding inhibition with a binding half-life of 2.5 h and an inhibition constant (K_i^*) of 1.6(± 0.7) pM. Even though NeuNAc oxime binds NeuB with high affinity, there remains approximately 10% residual activity even after extended pre-incubation with high inhibitor concentrations. In contrast, in the presence of substrates, when NeuB was actively catalyzing NeuNAc synthesis, complete inhibition by NeuNAc oxime was observed within 6 h. This inhibition profile is similar to NH_2OH; which has previously been shown to elicit complete, time-dependent inhibition. We propose the existence of two NeuB conformations: an asymmetric idle state conformation ($NeuB^{IS}$), in which NeuNAc oxime is able to bind to only one monomer of this dimeric enzyme, and a second conformation, running state NeuB ($NeuB^{RS}$), which is completely inhibited due to either NeuNAc oxime binding to the second monomer, or the dimer adopting a conformation in which the unbound monomer is inactive. Experiments with [1-^{14}C]PEP showed that in the presence of large excess of substrate, inhibition occurred faster than with a lower excess. This suggests that a sustained buildup of $NeuB^{RS}$ is required for complete inhibition.

Acknowledgements

I would like to take this opportunity to thank my supervisor Dr. Paul Berti for giving me the opportunity to study in his laboratory, for guiding me, and for always being supportive. Although the research was not always easy, I can truly say that this experience helped me mature as a scientist and as a person. The skills and knowledge that I have acquired during this time are invaluable assets which I will continue to use throughout my life. Further, I would like to thank my committee members Dr. Russell Bishop and Dr. Nathan Magarvey for their valuable suggestions and guidance.

I would like to also thank my lab members Naresh Balachandran, Vincent Azhikannickal, Shan Jiang, Jason Thomas, Vamana Rajeswaran, Lauren Wilson, Xiaoyi Ji, Peter Kim, Jenny Zheng, Adam Mepham, Rasa Bakhtiari, Morooj Ba-Akdah, and Simanga Gama. You guys were a joy to work with, and above all, you were great friends. I won't forget you guys! I am especially thankful to Naresh for answering all my theoretical questions throughout the years; to Vince for helping me create some of the figures in this thesis; and to Shan for putting up with my pranks.

Захваљујем се својим родитељима за сталну подршку и помоћ. Без вас неби ништа било могуће. Захваљујем се дјевојци Зорици за њезину љубав и за њезино разумјевање. Хвала ти што си увијек била уз мене. Морам исто да се захвалим пријатељима Вањи Мишићу, Бранку Маринићу, Младену Ђукићу, и Игору Драгојевићу. Ви сте увијек били ту за добар провод и право дружење.

Table of Contents

Abstract iii
Acknowledgements iv
Table of Contents v
List of Abbreviations vii
Table of Figures ix
List of Tables xi

1 Introduction 1

1.1 Sialic acids 1

1.1.1 Structure and function 1
1.1.2 Bacterial use 2
1.1.3 Biosynthesis 4

1.2 NeuB homologues: KDO8P and DAH7P synthases 5
1.3 Bacterial sialic acid synthase (NeuB) 6

1.3.1 Catalytic mechanism 6
1.3.2 Crystal structure 10

1.4 Enzyme inhibition and transition state theory 12
1.5 Slow-binding inhibition 15
1.6 Inhibition of NeuB and KDO8P/DAH7P synthases 17

2 Objective of study 22

3 Materials and methods 23

3.1 NeuB 23
3.2 Determining substrate binding kinetics for NeuB 23
3.3 Synthesis and purification of NeuB inhibitors 24
3.4 Inhibition of NeuB for kinetic studies 25
3.5 Synthesis of [1-^{14}C]NeuNAc 25
3.6 Synthesis of [1-^{14}C]NeuNAc oxime 26
3.7 Synthesis of [1-^{14}C]PEP 26
3.8 Tracking NeuB inhibition with [1-^{14}C]PEP 27
3.9 NeuNAc oxime inhibition during catalysis 28
3.10 Data analysis 29

4 Results 30

4.1 NeuB substrate binding kinetics 30
4.2 Synthesis and characterization of NeuB inhibitors 31
4.3 Exploring inhibitory properties of NeuNAc oxime 34
4.4 The connection between NH_2OH and NeuNAc oxime inhibition 36
4.5 Binding of [1-^{14}C]NeuNAc oxime to NeuB 37
4.6 Tracking NeuB inhibition with [1-^{14}C]PEP 38
4.7 NeuNAc oxime inhibition during catalysis 40

5 Discussion 43

5.1 NeuB substrate binding kinetics 43
5.2 NeuNAc oxime inhibition kinetics 45
5.3 Tracking NeuB inhibition with [1-^{14}C]PEP 47
5.4 NeuNAc oxime inhibition during catalysis 51
5.5 Residual activity 53

6 Conclusion and future work 56

7 References 59

List of Abbreviations

A5P:	D-arabinose-5-phosphate
AFPIII:	Type III antifreeze protein
CP:	Capsular polysaccharide
cpm:	Radioactive counts per minute
DAH7P:	2-keto-3-deoxy-D-arabino-heptulosonate-7-phosphate
E4P:	D-erythrose 4-phosphate
E•I:	Enzyme-inhibitor complex
E^{*}•I:	Isomerized enzyme-inhibitor complex
FRET:	Fluorescence resonance energy transfer (FRET)
GBS:	Guillian-Barré syndrome
IDA:	Iminodiacetic acid
KDN:	2-keto-3-deoxynonic acid
KDO8P:	2-keto-3-deoxy-D-*manno*-octulosonate-8-phosphate
K_i:	Inhibition rate constant
k_{inact}:	Rate of enzyme inactivation
k_{off}:	Rate constant for dissociation of inhibitor
k_{on}:	Rate constant for binding of inhibitor

LDH:	Lactate dehydrogenase
ManNAc:	*N*-acetylmannosamine
mBBr:	Monobromobimane
MurA:	enolpyruvyl UDP-GlcNAc synthase
N-CAM:	Neural cell adhesion molecule
NeuB:	NeuNAc or sialic acid synthase
$NeuB^{IS}$:	Non-catalyzing NeuB or idle state NeuB
$NeuB^{RS}$:	Fully inhibited conformation of NeuB or running state NeuB
NeuNAc:	*N*-acetylneuraminic acid
NH_2OH:	Hydroxylamine
NTA:	Nitrilotriacetic acid
PEP:	Phosphoenolpyruvate
ppSA:	Phosphoenolpyruvate synthase
PSA:	Polysialic acid
rManNAc:	Reduced ManNAc
THI:	Tetrahedral intermediate
TS:	Transition state
UDP-GlcNAc:	UDP-*N*-acetylglucosamine

Table of Figures

Figure 1. Neuraminic acid and its derivatives, NeuNAc and KDN 1

Figure 2. Bacterial and mammalian biosynthesis of the sialic acid, NeuNAc. 4

Figure 3. NeuB homologues: KDO8P and DAH7P synthases. 6

Figure 4. Two proposed NeuB reaction mechanisms. C-O bond cleavage and P-O bond cleavage 7

Figure 5. Proposed mechanisms for the formation of the THI during NeuNAc synthesis in NeuB. 9

Figure 6. Crystal structure of the NeuB with substrates. 11

Figure 7. NeuB active site architecture showing PEP, rManNAc, and Mn^{2+} 11

Figure 8. Reaction coordinate diagram showing the change in free energy (ΔG) during an uncatalyzed and catalyzed reaction 14

Figure 9. Slow-binding inhibitors 16

Figure 10. Progress curves for the inhibition of dihydrofolate reductase by a classical competitive inhibitor and a slow-binding inhibitor 16

Figure 11. The KDO8P and DAH7P oxacarbenium ion intermediates and three potent oxacarbenium mimic inhibitors for KDO8P synthase and DAH7P synthase 18

Figure 12. The KDO8P and DAH7P THIs and four THI mimic inhibitors for KDO8P synthase 19

Figure 13. The NeuB THI and oxacarbenium ion intermediate. A THI mimic inhibitor of NeuB and three oxacarbenium mimic inhibitors NeuNAc oxime, NeuNAc *O*-ethyl oxime, and NeuNAc *O*-fluoroethyl oxime. 19

Figure 14. Crystal structure of NeuNAc oxime bound in the active site of NeuB. ... 21

Figure 15. Steady state kinetic measurements for NeuB with ManNAc and PEP. ... 30

Figure 16. Relationship between $K_{M,Mn}$ and $[Ca^{2+}]$ 30

Figure 17. Tracking of NeuNAc *O*-fluoroethyl oxime synthesis on an anion exchange Mono-Q column....32

Figure 18. AV-200 MHz ^{19}F-NMR analysis of NeuNAc *O*-fluoroethyl oxime....32

Figure 19. AV-600 MHz ^{1}H-NMR analysis of NeuNAc *O*-fluoroethyl oxime....33

Figure 20. Inhibition profile of NeuNAc oxime with NeuB....35

Figure 21. NeuNAc oxime binding as a function of pre-incubation time....35

Figure 22. Inhibition of NeuB by NH_2OH in the presence of substrates is complete and time-dependent....36

Figure 23. Elution of NeuNAc, PEP and NeuB on an anion exchange Mono-Q column....38

Figure 24. Radioactivity trace of 10 min 500 nM NeuB reactions with 50 μM [1-^{14}C]PEP in the presence and absence of 63 mM NH_2OH....39

Figure 25. Radioactivity trace of 10 min 250 and 500 nM NeuB reactions with 10 μM [1-^{14}C]PEP in the presence and absence of 63 mM NH_2OH....39

Figure 26. The rate of NeuB inactivation in the presence and absence of NeuNAc oxime over 6 h....41

Figure 27. Two proposed mechanisms of NeuB inhibition in the presence of substrates and NH_2OH....50

Figure 28. NeuB inhibition mechanism by NeuNAc oxime in the presence of substrates....52

Figure 29. Slow-binding inhibitors and residual activity....54

Figure 30. Strategy for introducing a thiol-reactive FRET pair to detect movement of the NeuB antifreeze-like domain....58

List of Tables

Table 1. Extent of NeuB inhibition by NeuNAc oxime when pre-incubated with two of its substrates at 37°C for 6 h. 42

Table 2. Previously reported K_M and k_{cat} values for NeuB at pH 8.3 in comparison with our findings. 43

Table 3. Relative *in vitro* NeuB activation by various divalent metal co-factors 44

1 Introduction

1.1 Sialic acids

1.1.1 Structure and function

Sialic acids are a family of over sixty nine-carbon sugars derived from neuraminic acid (Figure 1). Sialic acids contain a carboxyl group at position 1, which gives it a pK_a of 2.2 and a negative charge under physiological conditions.[1]

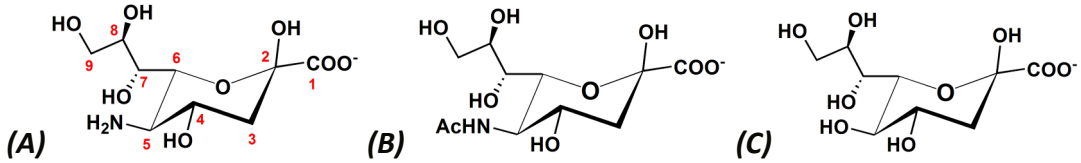

Figure 1. A) Neuraminic acid and its derivatives B) NeuNAc and C) KDN, two of the most common sialic acids in nature.

Although neuraminic acid itself does not occur in nature, its various derivatives do.[1] Two common derivates are *N*-acetylneuraminic acid (NeuNAc) and 2-keto-3-deoxynonic acid (KDN), which contain an acetyl and hydroxyl group at C5, respectively (Figure 1). Further modifications to neuraminic acid can occur at positions C4, C7, C8, and C9 with acetate, lactate, sulphate, phosphate, and methyl ethers. In mammals and a few Gram-negative bacteria, sialic acids are primarily located on the distal ends of cell surface glycoconjugates. In mammalian cells, sialic acids act either as biological targets[2] (i.e., ligand) or biological masks.[3] Their principle function is related to cellular and molecular recognition, which includes aiding the immune system in distinguishing between host and foreign cells/proteins based on their surface sialylation pattern. This is supported by the

fact that desialylation of host cells often leads to an autoimmune response.[4] Sialic acids are also integral to masking cells and molecules; influencing their degree of interactions with receptor proteins and pathogenic and non-pathogenic bacteria, viruses, and protozoa.[5] For example, the coating of mammalian erythrocytes by sialic acid influences their life span. Removal by serum sialidase (requiring approximately 120 days), exposes the penultimate galactose residues on the cell surface, enables their recognition by galactose-specific receptors on phagocytes, and promoted degradation of the erythrocyte cells.[6] Removal of malignant cells follows a similar mechanism; however, it is for this reason that these cells are hyper-sialylated. This protects them from the immune system and promotes malignancy.[7] Sialic acids are also responsible for the binding and transport of positively charged molecules such as Ca^{2+} and the "slimy" character of mucous coated surfaces.[1]

1.1.2 Bacterial use

Certain strains of neuroinvasive, Gram-negative bacteria such as *Escherichia coli* K1, *Campylobacter jejuni*, and *Neisseria meningitidis* can produce and display NeuNAc on their cell surface in order to mimic mammalian cells and evade the immune system by hiding their antigenic sites.[1] *Neisseria meningitidis*, responsible for worldwide epidemic meningitis, is an upper respiratory pathogen that causes inflammation of the protective tissue surrounding the brain and spinal cord. Thirteen *N. meningitidis* serogroups exist; 6 of which are considered life-threatening (A, B, C, W-135, X, and Y).[8] Only serogroup B produces a linear homopolymer of up to 200 α-(2→8)-linked NeuNAc known as

polysialic acid (PSA), on its capsular polysaccharide (CP). Bacteria possessing PSA are commonly known to infect the upper respiratory and intestinal tract of humans. *E. coli* K1 also contains PSA on its CP. This bacterium infects the lower intestinal tract, causing irritable bowel syndrome, septic shock, and meningitis.[9] It is the leading cause of meningitis in premature infants.[10] PSA is also found on the surface of the mammalian neural cell adhesion molecule, N-CAM, which is a widespread membrane glycoprotein that regulates cell-cell adhesion and is involved in neurite growth and learning.[11-12] Creation of antibodies against PSA would therefore stimulate a host autoimmune response.[13] N-CAMs with longer PSA chains, typically found in embryonic neural tissue, are most vulnerable during an autoimmune response caused by meningococci infections.[12] Currently, vaccination is the only reliable means to control meningitis, but vaccines do not exist for serogroup B for two reasons: 1) poor immune response and 2) risk of autoimmune induction.[13]

Campylobacter jejuni is the most common cause of bacterial gastroenteritis in humans. It has also been linked to Guillian-Barré syndrome (GBS) – an autoimmune disorder affecting the peripheral nervous system and causing neuromuscular paralysis.[14] Structural analysis of lipopolysaccharides (LPS) on the surface of certain *C. jejuni* strains has shown remarkable similarity with human gangliosides; which are prevalent in both the central and peripheral nervous systems.[15] It is believed that the cause of the autoimmune response in patients experiencing GBS results from anti-ganglioside antibodies that are created in response to *C. jejuni* infections.[15]

1.1.3 Biosynthesis

NeuNAc biosynthesis follows similar routes in bacteria and mammals (Figure 2).[16]

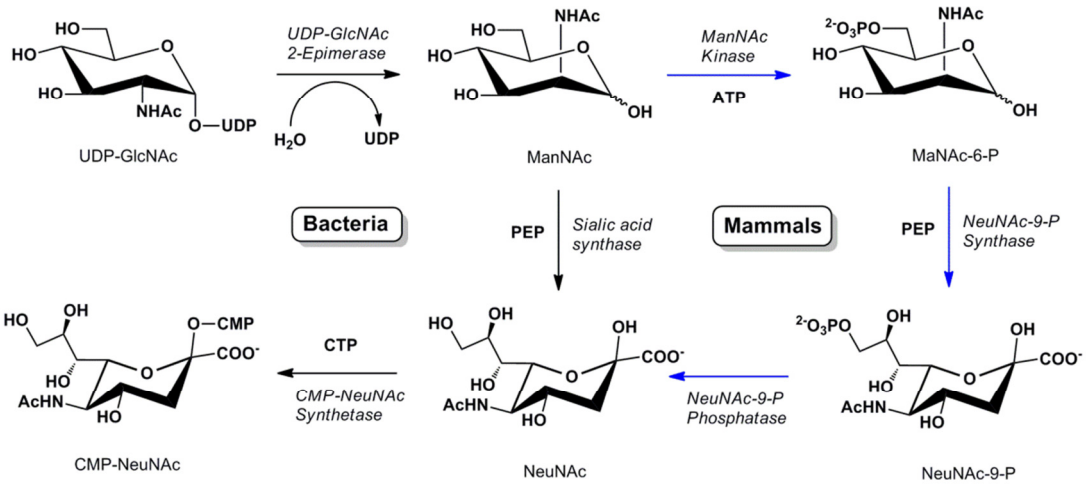

Figure 2. Bacterial (black) and mammalian (blue) biosynthesis of the sialic acid, NeuNAc.

The first committed step is catalyzed by the enzyme UDP-*N*-acetyl-glucosamine 2-epimerase, which inverts the stereochemistry at C2 and hydrolyzes the glycosidic phosphate bond in converting UDP-*N*-acetylglucosamine (UDP-GlcNAc) to *N*-acetylmannosamine (ManNAc).[16] The mammalian UDP-GlcNAc 2-epimerase then phosphorylates ManNAc while the bacterial enzyme does not. In mammals, NeuNAc-9-phosphate synthase catalyzes the condensation of phosphoenolpyruvate (PEP) with ManNAc-6-P, generating NeuNAc-9-P. The bacterial enzyme, sialic acid synthase (NeuB) catalyzes a similar condensation of ManNAc and PEP to generate NeuNAc. The pathways then converge at the production at CMP-NeuNAc. CMP-NeuNAc is an activated form of NeuNAc that is used by CMP-sialyl transferases to synthesize PSA

chains. NeuB stands out as a drug target because it is unique to the bacterial pathway and it uses a different substrate than its mammalian analogue.[16] Inhibiting this enzyme would stop bacterial sialic acid biosynthesis while the mammalian pathway remains uninterrupted.

1.2 NeuB homologues: KDO8P and DAH7P synthases

Two major NeuB homologues that catalyze related reactions exist, 2-keto-3-deoxy-D-*manno*-octulosonate-8-phosphate (KDO8P) synthase and 2-keto-3-deoxy-D-arabino-heptulosonate-7-phosphate (DAH7P) synthase. All three enzymes are α-carboxyketose synthases that catalyze condensation reactions between PEP and an aldose (Figure 3). KDO8P synthase condenses PEP and D-arabinose-5-phosphate (A5P) to form KDO8P [17], an essential building block of the inner core of Gram-negative LPS.[18] DAH7P synthase condenses PEP and D-erythrose-4-phosphate (E4P) to form DAH7P. This reaction is the first committed step in the shikimate pathway for biosynthesis of aromatic compounds in microorganisms and plants.[19] Despite < 10% sequence identity between NeuB and KDO8P/DAH7P synthases, these homologues are mechanistically and functionally similar. As will be demonstrated, studies on KDO8P and DAH7P synthases have proven useful in the study of NeuB.

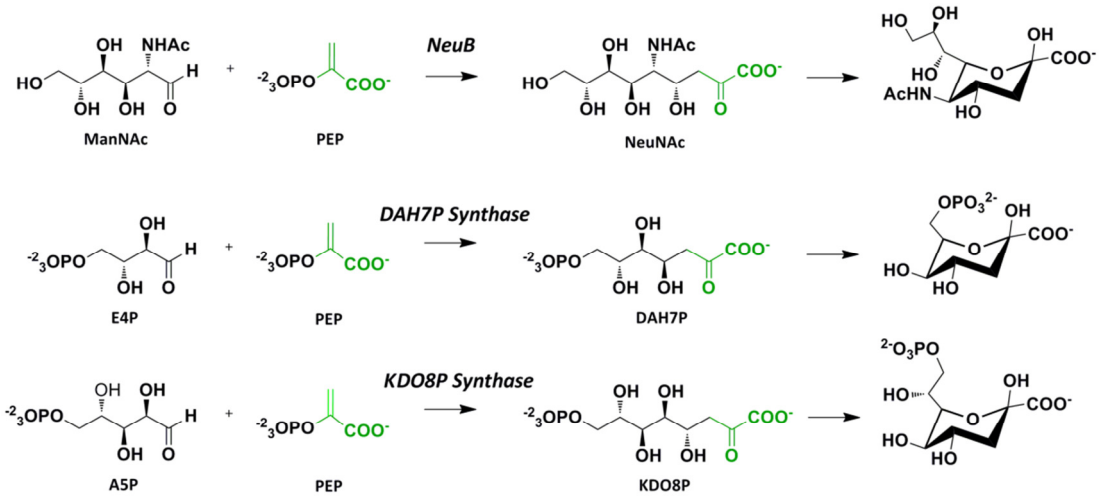

Figure 3. NeuB homologues, KDO8P and DAH7P synthases, catalyze very similar PEP condensation reactions with an aldose. The linear product spontaneously cyclizes in solution.

1.3 Bacterial sialic acid synthase (NeuB)

1.3.1 Catalytic mechanism

NeuB catalyzes the condensation of PEP with ManNAc in the presence of a divalent cation, showing highest activity with Co^{2+} and Mn^{2+}.[20] Two mechanisms have been proposed for NeuB, which are characterized by cleavage of either the C2-O2 bond or the O2-P bond of PEP (Figure 4).[16] The C-O bond cleavage mechanism involves attack by C3 of PEP onto the carbonyl carbon of ManNAc. The resulting oxacarbenium ion would subsequently be attacked by a water molecule to generate a tetrahedral intermediate (THI). Finally, phosphate would be lost to give the open-chain form of NeuNAc which would spontaneously cyclize in solution (Figure 4A). The P-O bond cleavage mechanism involves an initial attack by water at the PEP phosphorous to give free phosphate and an

enolate species. This enolate species would then attack the carbonyl carbon of ManNAc to generate the open-chain form of NeuNAc (Figure 4B). To distinguish between these two mechanisms, ^{18}O-labeled PEP was reacted with *N. meningitidis* NeuB. The ^{18}O-label was retained in the phosphate product ($H^{18}OPO_3^{2-}$) demonstrating that the reaction occurred via C-O bond breakage.[21] This mechanism is also conserved in KDO8P and DAH7P synthases.[22-23] In fact, direct evidence for the existence of the THI in the KDO8P synthase reaction was shown using time of flight electrospray ionization mass spectrometry.[24]

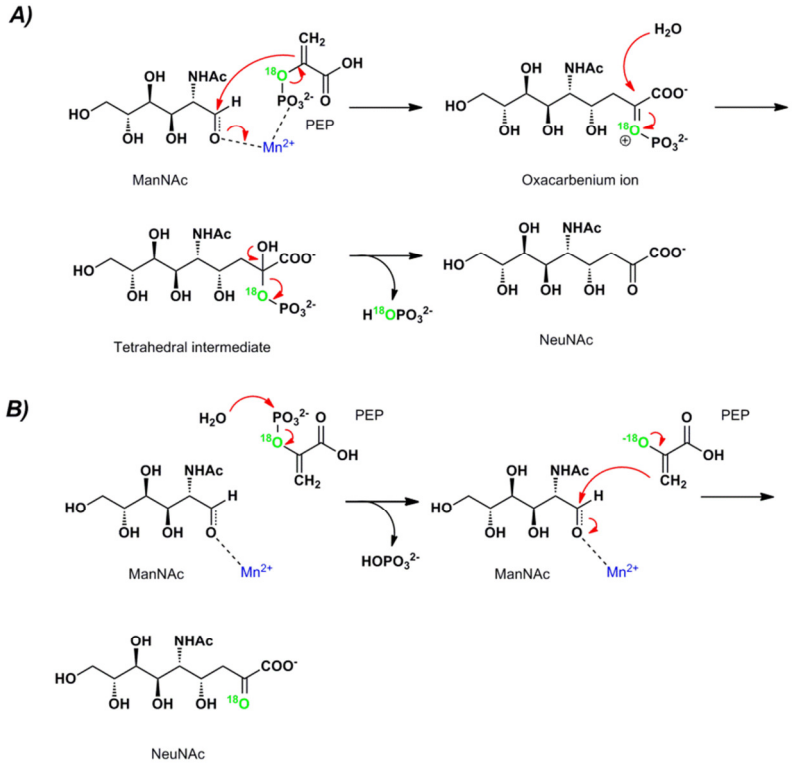

Figure 4. Two proposed NeuB reaction mechanisms. A) C-O bond cleavage and B) P-O bond cleavage. ^{18}O-labeled (green) PEP was used to determine that the mechanism occurs via C-O bond cleavage.

Formation of the THI by C-O bond cleavage can also occur in two ways (Figure 5). The first mechanism involves attack by C3 of PEP onto the carbonyl carbon of ManNAc to generate a transient oxacarbenium ion, which undergoes nucleophilic attack by water to form the THI (Figure 5A). The second mechanism involves a deprotonated water molecule attacking C2 of PEP. The resulting carbanion then attacks the carbonyl carbon of ManNAc to form the THI (Figure 5B). The exact route by which THI formation occurs in NeuB is still undetermined. However, Clark, *et al.* showed that an unactivated enolpyruvyl group is not susceptible to nucleophilic attack.[25] This suggests that the formation of a PEP carbanion species is highly unlikely. Further evidence for the formation of an oxacarbenium ion will be discussed later.

The recent discovery that the NeuB THI bears a (2*R*)-configuration, indicates that the water-derived hydroxide is delivered to the *si* face of the oxacarbenium ion. This water molecule appears to be activated by the metal co-factor. This suggests that the metal has two catalytic roles. First, it acts as an electrostatic catalyst of the ManNAc C1 carbonyl group. Second, it activates the water nucleophile for addition onto the *si* face of the oxacarbenium ion.[26] Other studies with have shown that NeuB activity increased as the concentration of Mn^{2+} is raised from 0.2 – 1 mM. This reflects the dependence of NeuB for a divalent metal co-factor. However, at higher concentrations of Mn^{2+}, NeuB activity decreased. This is most likely a result of non-productive metal binding to an allosteric site on the enzyme, which has previously been shown to decrease the affinity of substrates for the active site.[27-28]

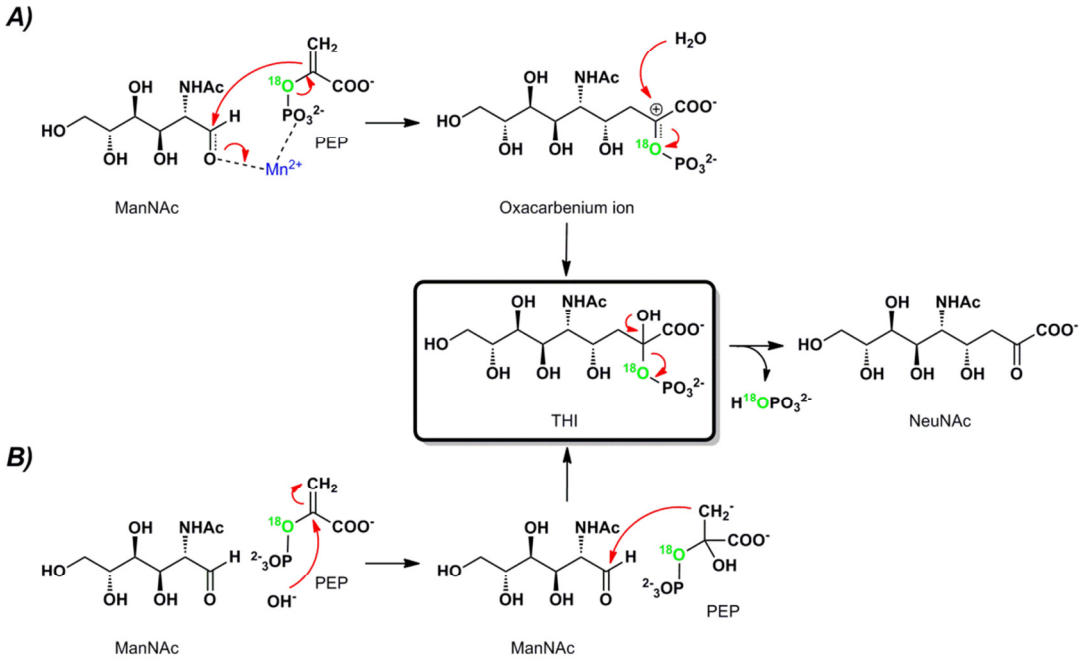

Figure 5. Proposed mechanisms for the formation of the THI during NeuNAc synthesis in NeuB. A) The enolate form of PEP attacks ManNAc to generate a transient oxacarbenium ion. B) Hydroxide attacks PEP to generate a carbanion which attacks ManNAc.

Additional studies were aimed at determining the stereospecificity of PEP addition. ^{1}H-NMR analysis has shown that *Z*- and *E*-[3-^{2}H]PEP produced [3*S*-^{2}H]NeuNAc and [3*R*-^{2}H]NeuNAc, respectively. These results show that the *si* face of PEP adds to the *si* face of ManNAc.[29] This differs in KDO8P and DAH7P synthase reactions, where the *si* face of PEP adds onto the *re* face of the aldose.[30]

1.3.2 Crystal structure

NeuB is a domain-swapped homodimer in solution (Figure 6B), with 349 amino acids and a molecular weight of 38 kDa per monomer. Each monomer consists of two domains joined by a linker region (residues 274 – 284).[21] The larger *N*-terminal domain (residues 1 – 273) contains the active site and resembles a classic $(\alpha/\beta)_8$ TIM barrel, with 8 parallel β-strands enclosed by 8 α-helices. This domain is also found in KDO8P and DAH7P synthases, suggesting that all three enzymes share common active site architecture.[31-32] The smaller *C*-terminal domain (residues 285 – 349) is a "pretzel-shaped" fold closely related to type III antifreeze proteins (AFPIII) found in eel pouts (Figure 6A).[21] This domain is not found in other PEP-utilizing enzymes such as KDO8P and DAH7P synthases. In NeuB, the type III antifreeze domain is responsible for capping the active site of the neighbouring monomer as well as donating a residue, Arg314, to it. In the crystal structure reported by Gunawan *et al.*, the active site contains Mn^{2+}, PEP, and reduced ManNAc (rManNAc) (Figure 7), whose spatial geometry suggests that it is positioned to act as an electrophilic catalyst, polarizing the ManNAc carbonyl carbon prior to PEP attack. This is also consistent with the C-O bond cleavage mechanism. However, it is still not fully clear whether the role of the metal is catalytic or structural. It has been shown that metal-dependent KDO8P synthase can be mutated to become metal-independent.[29] This suggests that the role of the metal is a structural one. In addition, the *si* face of PEP faces the *si* face of rManNAc, supporting the previously observed stereochemistry of addition.

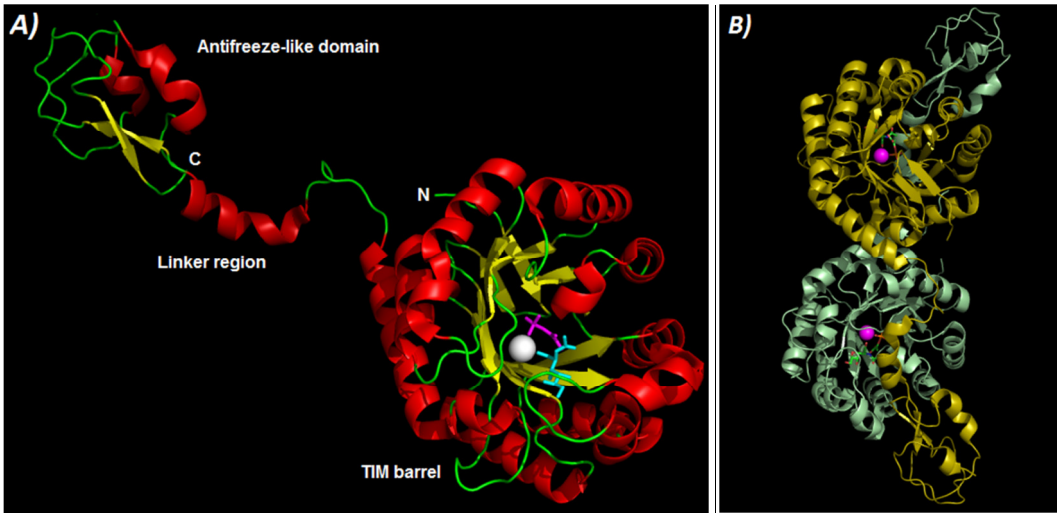

Figure 6. A) Crystal structure of the NeuB monomer (PDB: 1XUZ) showing the *C*-terminal antifreeze-like domain, the linker region, and the *N*-terminal TIM barrel.[21] The active site is occupied by Mn^{2+} (gray), PEP (magenta) and rManNAc (cyan). B) Overall crystal structure of the NeuB domain-swapped dimer. Monomers are shown in gold and cyan.

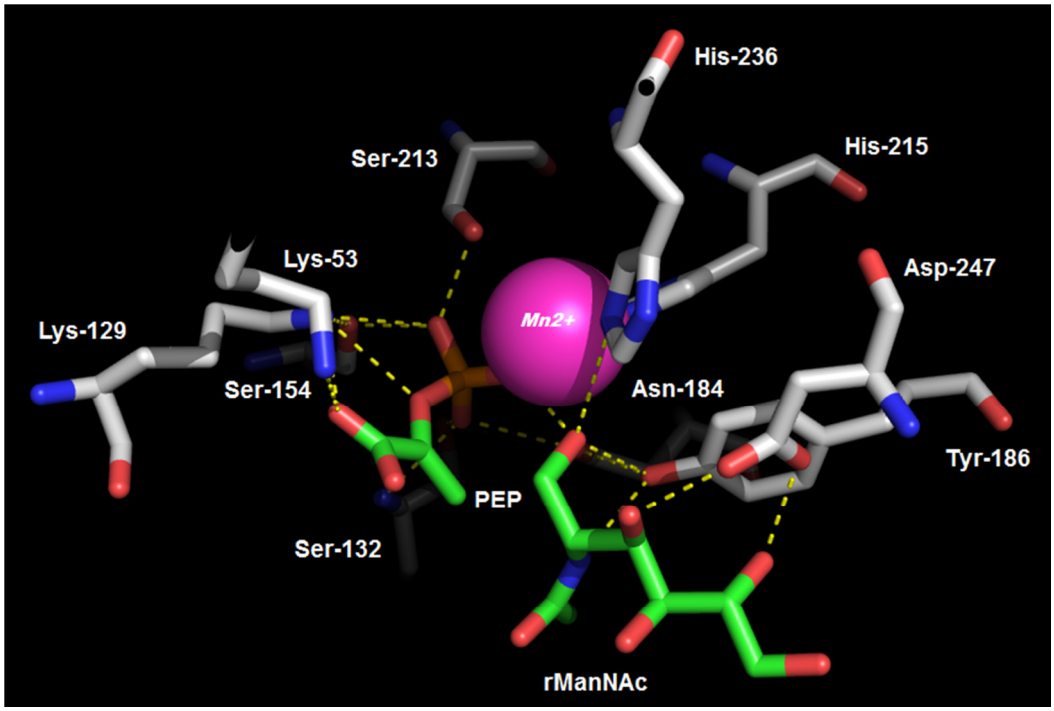

Figure 7. NeuB active site architecture showing PEP, rManNAc (green), and Mn^{2+} (magenta) being bound by key residues (gray). Hydrogen bonds are shown as yellow dashes (PDB: 1XUZ).[21]

Potential hydrogen bonding interactions can occur between the PEP phosphate group and Ser132, Ser154, Ser213, and Asn184. PEP can be further stabilized by interactions between its carboxyl group and Lys53 and Lys129. This suggests that PEP is bound in a fully ionized form, which would further argue against the formation of a carbanion during THI formation. Evidence for an oxacarbenium intermediate also exists due to the anionic amino acids (Glu25, Glu134, Glu234) surrounding C2 of PEP, which would aid in stabilizing this species.[21]

1.4 Enzyme inhibition and transition state theory

Enzyme inhibitors are substances capable of slowing the rate of an enzyme-catalyzed reaction.[33] They can serve as drugs, as well as probes in the study of enzyme mechanisms. The three main modes of non-covalent inhibition are: competitive, non competitive, and uncompetitive. All three classes bind to enzymes reversibly (i.e., via non-covalent interactions).

Competitive inhibitors generally resemble the chemical structure and molecular geometry of the substrate(s), and thereby compete with the substrate for binding in the active site. Such inhibition is characterized by i) dependence upon the concentration of the inhibitor and substrate as well as their relative affinities for the enzyme (K_i and K_M), ii) inhibitor binding to free enzyme but not to the enzyme-substrate complex, and finally, iii) increased apparent K_M and unaltered V_{MAX} when inhibitor is present.[34]

Non-competitive inhibitors usually do not occupy the active site. Instead, they are able to influence catalysis by binding to an allosteric site on the enzyme and inducing a conformational change that alters the shape of the active site. Hence, their binding is influenced by neither substrate concentration nor the K_M value. Non-competitive inhibitors do not alter the K_M value; they do, however, lower the apparent V_{MAX} since they are able to hamper catalysis by distorting the active site.[34]

Uncompetitive inhibitors are only able to bind the enzyme-substrate complex. These inhibitors generally tend to hinder the release of the enzyme-catalyzed product, thereby decreasing V_{MAX}. The K_M value is also decreased due to loss of the enzyme-substrate complex from the equilibrium.[34]

Inhibition of multi-substrate enzyme systems is more difficult to analyze. Such enzymes can catalyze sequential or ping pong reactions. Sequential reactions involve the binding of all substrates to an enzyme prior to catalysis and release of products; whereas in ping pong reactions some of the chemical steps occur, and one or more products are released before all the substrates have bound. Sequential reactions can involve ordered or random binding of substrates.[33] The mode of multi-substrate binding is important when determining the overall steady-state rate equation for inhibition. Further, the mode of inhibition can vary with respect to each substrate in multi-substrate enzyme systems. For example, an inhibitor which is competitive against one substrate can be uncompetitive against the other substrate. This occurs when the inhibitor combines with one substrate in the active site and then competitively hinders the binding of the other substrate.[35]

Transition state mimics are a class of inhibitors designed to mimic the structure and charge distribution of the transition state (TS).[36] The TS is the highest energy point on the lowest energy path between reactants and products. The hurdle for any enzymatic reaction is the high energy needed to reach the TS between substrates and products (Figure 8). Enzymes increase reaction rates by tightly binding to, and therefore stabilizing the TS. This lowers the free energy of the TS and decreases the energy barrier between substrates and products.[36]

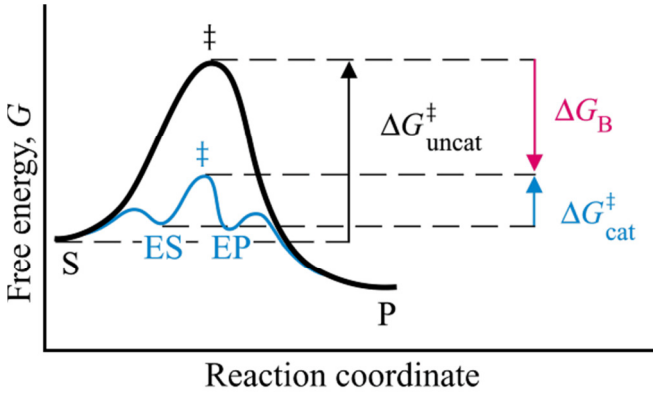

Figure 8. Reaction coordinate diagram showing the change in free energy (ΔG) during an uncatalyzed and catalyzed reaction. Enzymes increase reaction rates by decreasing the free energy associated with the unstable TS (‡). $\Delta G^{‡}_{uncat}$ and $\Delta G^{‡}_{cat}$ represent the free energy required for the uncatalyzed and catalyzed conversion of substrate to product, respectively. ΔG_B is the difference between $\Delta G^{‡}_{uncat}$ and $\Delta G^{‡}_{cat}$. ES is the enzyme-substrate complex and EP is the enzyme-product complex. From reference [37].

The advantage of creating inhibitors that mimic the TS as opposed to the substrate, is that enzymes bind the TS up to 10^{20} times tighter.[38] The challenge in creating TS inhibitors is that the enzyme mechanism and TS structure must be well characterized. This is difficult given the fact that TS have very short lifetimes (~10^{-13} s).[39] In the case of NeuB and KDO8P/DAH7P synthase, the identity of the TS is unknown. However, the fact that the

C-O bond is cleaved in the NeuB reaction and studies on KDO8P and DAH7P synthases have shed additional light on the mechanisms of these enzymes.[22-24,30] Of particular importance is evidence for the existence of two intermediate species, the THI and oxacarbenium ion; which can be used as models for inhibitors. The THI is a stable intermediate whose mimic can be used as a mechanistic probe. The oxacarbenium ion is an unstable and reactive intermediate with similar geometry and charge distribution to the presumed TS structures; its mimics have potential to be both probes and powerful inhibitors.

1.5 Slow-binding inhibition

Slow-binding inhibitors are compounds that inhibit their target in a time-dependent manner; often attaining the equilibrium between enzyme, inhibitor and enzyme-inhibitor complex (E•I) in the second to minute time scale.[35] They often require the pre-incubation of a high ratio of inhibitor to enzyme. In cases where inhibition occurs with an approximately equal ratio of enzyme and inhibitor, it is said to be slow, tight-binding.[35] Slow-binding inhibitors differ from classical inhibitors in that they bind weakly in the initially formed E•I complex. However, tighter binding is achieved following a slow conformational isomerisation of E•I to E^{*}•I (Figure 9). Slow-binding inhibitors can have either fast or slow k_{on} rates, but always slow k_{off} rates as $k_{off} = k_{on} \times K_i$. Release of I from E^{*}• I can take minutes to days.[40] TS analogs are often slow-binding inhibitors because they are thought to bind a TS-like conformation of the enzyme more tightly than the

ground state conformation.[41] It therefore follows that slow-binding inhibitors have two important pharmaceutical benefits: 1) longer inhibition due to slow k_{off} rates and hence less overall drug consumption and 2) upstream build-up of substrates will not counter any inhibitory effects since the E^*•I complex is not recognized by substrates.[40]

$$E + I \overset{\text{fast}}{\rightleftharpoons} E\cdot I \overset{\text{slow}}{\rightleftharpoons} E^*\cdot I$$

Figure 9. Slow-binding inhibitors lead to a slow isomerization of the initially formed E•I in order to generate the tightly-bound E^*•I complex. Release of inhibitor from E^*•I can take minutes to days.

The progress curves for enzyme inhibition by a classical competitive inhibitor and a slow binding inhibitor (Figure 10). Slow-binding inhibitors are characterized by an initial burst of reaction followed by a slow steady-state rate.[40] The initial burst reflects the weak binding between the inhibitor and the ground state enzyme conformation. Once the enzyme conformation has adjusted to the inhibitor, tight binding is observed.

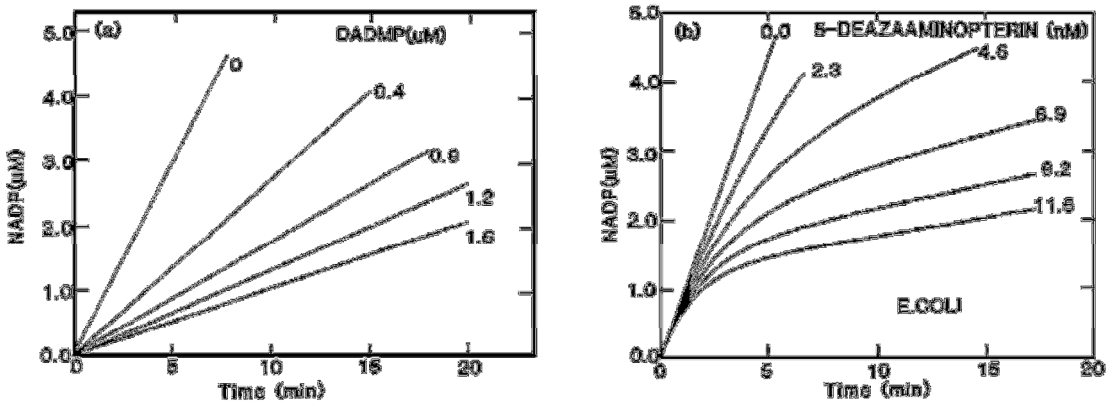

Figure 10. Progress curves for the inhibition of dihydrofolate reductase by A) a classical competitive inhibitor, 2,4-diamino-6,7-dimethylpteridine (DADMP) and B) a slow-binding inhibitor, 5-deazaaminopterin. From reference [40].

Progress curves for slow-binding inhibitors can be fitted to the 'burst equation' (Equation **1**). This equation is valid under the assumption that depletion of substrates is negligible.[42]

$$[\mathrm{P}]_t = v_s t + \frac{(v_0 - v_s)(1 - e^{-kt})}{k} \quad \textbf{(1)},$$

where P is the concentration of product at time t, k is the apparent first-order rate constant for reaching the steady-state velocity, and v_0 and v_s are the initial and steady-state velocities.

1.6 Inhibition of NeuB and KDO8P/DAH7P synthases

Inhibition of DAH7P and KDO8P synthases has previously been explored.[18,43-46] These studies have primarily focused on mimicking the THI and oxacarbenium ion. In 1999, Du *et al.* synthesized an oxacarbenium mimic inhibitor, **1** (K_i = 0.4 μM) (Figure 11).[43] Inhibitor **1** was co-crystallized with KDO8P synthase and shown to bind in the active site.[18] A hydrolytically stable analog of this inhibitor was later synthesized, **2**, in hopes of improving its antibacterial properties. However, both **1** and **2** were unable to inhibit bacterial growth, presumably due to an inability to cross the bacterial cell membrane.[45] The inhibition studies on KDO8P synthase inspired the synthesis of the first DAH7P synthase inhibitor, **3**, which mimicked the DAH7P oxacarbenium ion.[46] A key modification in the noted inhibitors is the replacement of the phosphate monoester O-P bond by a stable phosphonate C-P bond. This ensures that phosphate cannot be expelled as a leaving group and that the inhibitor cannot be turned over.

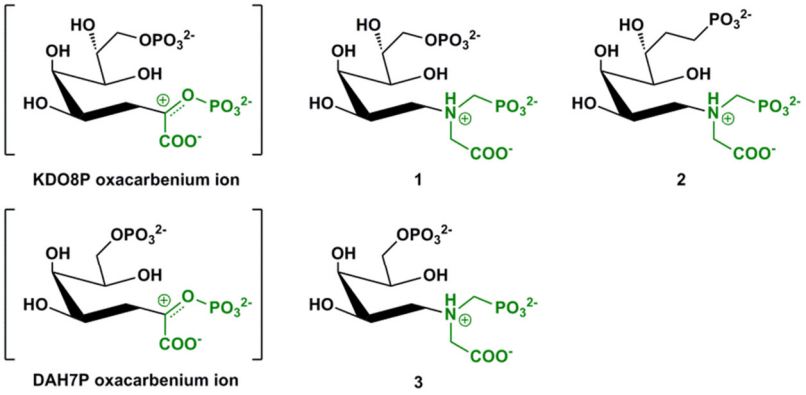

Figure 11. The KDO8P and DAH7P oxacarbenium ion intermediates and three potent oxacarbenium mimic inhibitors for KDO8P synthase (**1** and **2)** and DAH7P synthase, **3**. The K_i values of **1** and **2** are 0.4 and 50 μM, respectively. The IC_{50} value for **3** is 6.6 μM.

Grison *et al.* reported the first THI mimic inhibitors for both KDO8P and DAH7P synthases (Figure 12).[44] Disk diffusion tests were used to screen for antibacterial potency. Removing the terminal phosphate in **4**, **5**, **6**, and **7** reduces the negative charge to aid the inhibitors in crossing the cell membrane. This was further illustrated in **5** and **7**, where the phosphate monoester was converted to a neutral diethyl phosphonic ester. The inhibitors were tested on different Gram-negative and Gram-positive bacteria, with only **5** and **7** showing antibacterial activity. As expected, both **5** and **7** were effective against Gram-negative bacteria; whereas only **7** was effective against Gram-positive bacteria. Compound **5** lacks antibacterial activity against Gram-positive bacteria due to their lack of KDO8P synthase or an outer LPS layer. No K_i values were reported in the study.

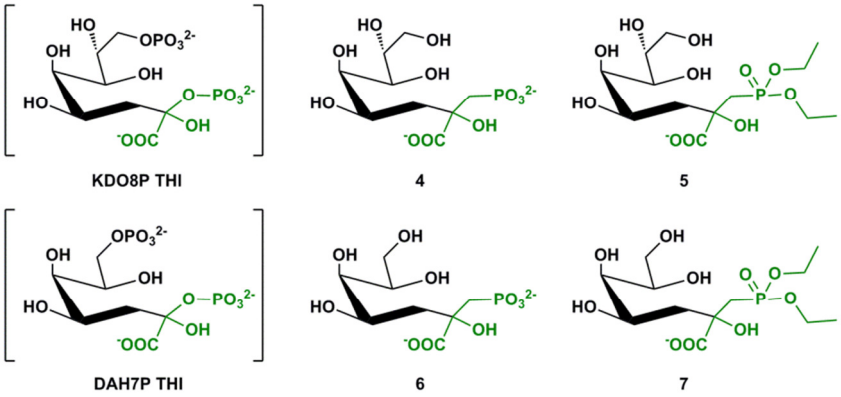

Figure 12. The KDO8P and DAH7P THIs and four THI mimic inhibitors for KDO8P synthase (**4** and **5**) and DAH7P synthase (**6** and **7**).

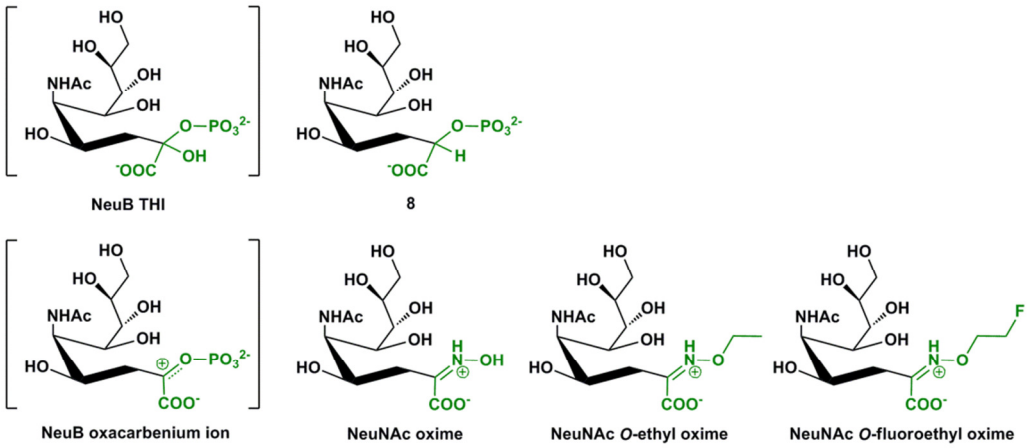

Figure 13. The NeuB THI and oxacarbenium ion intermediate. A THI mimic inhibitor of NeuB, **8**, has previously been reported. Three oxacarbenium mimic inhibitors are studied by our group, NeuNAc oxime, NeuNAc *O*-ethyl oxime, and NeuNAc *O*-fluoroethyl oxime.

The first published inhibitor of NeuB, **8**, is also a THI mimic inhibitor with a $K_i = 3.1(\pm 0.1)$ μM (Figure 13).[26] This inhibitor was soaked into NeuB crystals and shown to bind the active site in a (2*R*)-configuration, suggesting that the THI has the same configuration. Further, the authors have shown partial occupancy (50%) of Mn^{2+} in the NeuB•**8**•Mn^{2+} complex. This was attributed to a distorted Mn^{2+} octahedral

arrangement during binding of **8**.[26] All of the mentioned mimics showed slow-binding behavior; often requiring extensive pre-incubation of enzyme and inhibitor prior to observed inhibition.

Our group has chosen to design and test NeuB inhibitors that mimic the oxacarbenium ion intermediate. Since the oxacarbenium ion is less stable than the THI, and likely very close to the TS structure's geometry and charge, it is assumed that it will be better stabilized by the enzyme and therefore should produce a more powerful inhibitor. We propose three oxacarbenium mimic inhibitors for NeuB: NeuNAc oxime, NeuNAc *O*-ethyl oxime and NeuNAc *O*-fluoroethyl oxime (Figure 13). The role of NeuNAc oxime is that of a TS mimic that can provide clues to the actual TS of NeuB and a potential antibacterial compound. NeuNAc oxime was shown to be a potent and slow binding inhibitor of NeuB. Its binding is competitive with respect to ManNAc and PEP. However, residual enzyme rate is associated with this inhibitor. Interestingly, hydroxylamine (NH_2OH), a precursor in the synthesis of NeuNAc oxime, showed complete time-dependant inhibition of NeuB when added during enzyme catalysis.[47] This is believed to occur when NH_2OH reacts with the NeuB product, NeuNAc, in the active site. This leads to the *in situ* formation of NeuNAc oxime and, for an unknown reason, complete inhibition of NeuB. Our group has co-crystallized NeuB with NeuNAc oxime[47] (Adam Rosanally, unpublished data) (Figure 14). The inhibitor was bound in the *trans* conformation in both active sites in the dimer and was shown to mimic the previously

reported orientation and placement of ManNAc and PEP. The Mn^{2+} co-factor was absent in all crystal structures containing NeuNAc oxime.

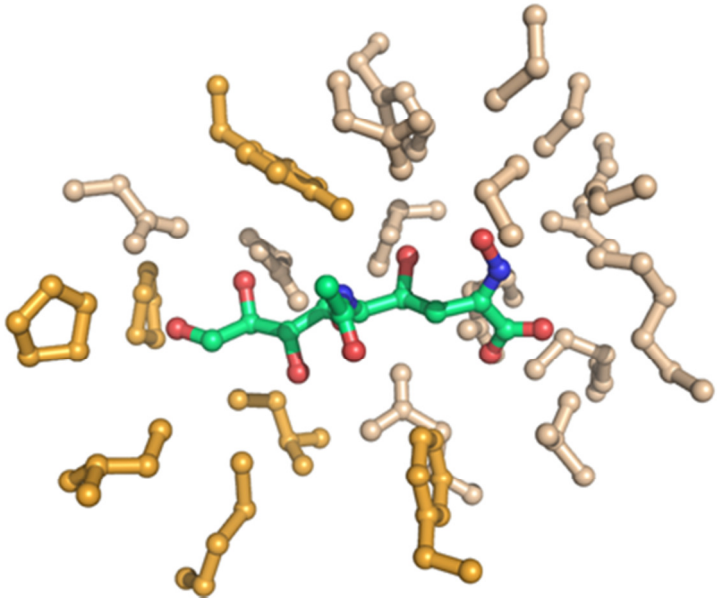

Figure 14. Crystal structure of NeuNAc oxime bound in the active site of NeuB.

The NeuNAc *O*-fluoroethyl oxime has potential as an imaging agent. Replacement of the F atom with ^{18}F could yield a radiopharmaceutical able to bind NeuB *in vivo* during *N. meningitidis* infection. This would offer a fast and highly specific means for diagnosis of bacterial meningitis. Lastly, NeuNAc *O*-ethyl oxime has been designed as a structural link between NeuNAc oxime and NeuNAc *O*-fluoroethyl oxime.

2 Objective of study

The objective of the following study was to further explore the inhibitory properties of NeuNAc oxime and NH_2OH. The mechanism by which these two compounds inhibit NeuB is of particular interest considering that they have complementary traits. NeuNAc oxime is a potent, time-dependent inhibitor which is unable to fully inhibit enzyme activity; whereas NH_2OH shows complete inhibition, but at millimolar concentrations. Understanding these mechanisms will answer important questions about NeuB inhibition and help in the later development of inhibitors for other α-carboxyketose synthases. The proposed *in situ* synthesis of NeuNAc oxime during NH_2OH inhibition was studied with radiolabelled PEP. We aimed to see the transfer of the radiolabel from PEP to NeuNAc and NeuNAc oxime. Trapping radiolabelled NeuNAc oxime with NeuB would validate this hypothesis and directly show that NeuNAc oxime is a mechanistic inhibitor of NeuB. We also revisited the inhibitory properties of NeuNAc oxime and, likewise, began testing the NeuNAc *O*-ethyl and *O*-fluoroethyl oxime inhibitors.

3 Materials and methods

3.1 NeuB

N-terminally His_6-tagged NeuB was expressed and purified as described previously.[47] NeuB activity was followed by detecting phosphate production using the Malachite Green/ammonium molybdate colorimetric assay in a 96 well plate format, as previously described.[47-48] NeuB was regularly demetallated with 1 mM EDTA (incubated overnight with 15 μM NeuB) in order to remove contaminating metals attained during purification.

3.2 Determining substrate binding kinetics for NeuB

In order to confirm the dependence of NeuB for its substrates and determine their respective K_M values, initial velocities were measured at 37°C using the Malachite Green assay with varying substrate concentrations. $K_{M,ManNAc}$ was determined with fixed 3 mM PEP, 1 mM $MnCl_2$, 100 μM tris(2-carboxyethyl)phosphine (TCEP), 0.1 mg/mL BSA, and 0 – 5 mM ManNAc in 50 mM Tris-OAc, pH 8.3. $K_{M,PEP}$ was determined under similar conditions, but with fixed 15 mM ManNAc and 0 – 3 mM PEP.

Because there was metal contamination of NeuB during the purification process and the fact that exhaustive demetallation irreversibly inactivated the enzyme, $K_{M,Mn}$ was measured in the presence of Ca^{2+}. Ca^{2+} bound residual EDTA and acted as a weak competitive inhibitor with respect to Mn^{2+} because it does not activate NeuB. NeuB was first demetallated with an overnight incubation with 2 mM EDTA. The bulk of the

EDTA was removed using a HiTrap Desalting (1.6 x 2.5 cm, GE Healthcare) column. $K_{M,Mn}$ was then determined by varying $MnCl_2$ concentrations in the presence of various $CaCl_2$ concentrations ranging from 100 μM to 10 mM. Assays were performed with 15 mM ManNAc, 3 mM PEP, 100 μM TCEP, 0.1 mg/mL BSA, and 0 – 5 μM $MnCl_2$ in 50 mM Tris-OAc, pH 8.3. We obtained the true $K_{M,Mn}$ value by plotting the different $K_{M,Mn}$ values against Ca^{2+} concentration. The y-intercept from this linear trend was indicative of the $K_{M,Mn}$ in the absence of Ca^{2+}.

3.3 Synthesis and purification of NeuB inhibitors

Synthesis of NeuNAc oxime was carried out by mixing hydroxylamine-HCl (200 mM) and NeuNAc (10 mM) and incubating for 48 h at room temperature, as described previously.[47] The NeuNAc *O*-ethyl oxime was synthesized similarly to the oxime inhibitor as described previously (Adam Rosanally, Biochemistry 4B06 thesis). The NeuNAc *O*-fluoroethyl oxime inhibitor was also synthesized similarly, using *O*-(2-fluoroethyl)-hydroxylamine hydrochloride synthesized by Karin Stephenson from John Valliant's laboratory.

Purification of all three inhibitors was performed on a Mono-Q (5x50 mm, GE Healthcare) column with a gradient of 0.8 – 80 mM ammonium acetate, pH 5.5, over 80 min. Following lyophilization, inhibitors were quantified using an acetone standard on ^{1}H-NMR and eventually stored in 50 mM Tris-OAc, pH 8.3, at -20°C.

3.4 Inhibition of NeuB for kinetic studies

Demetallated NeuB was pre-incubated for 20 h at 25°C with varying concentrations of NeuNAc oxime in fresh and filtered 50 mM Tris-OAc, pH 8.3. The pre-incubation mixture is used to start a reaction at 37°C containing 1.8 mM PEP and ManNAc, 2 mM $MnCl_2$, and 100 μM TCEP in 50 mM Tris-OAc, pH 8.3, such that the final concentration of NeuB was 150 nM. Initial velocities were measured for both inhibited NeuB and uninhibited controls that were pre-incubated under the same conditions.

3.5 Synthesis of [1-^{14}C]NeuNAc

[1-^{14}C]NeuNAc synthesis was carried out using NeuNAc aldolase (0.004 U/μL) (Sigma Aldrich), 10 mM [1-^{14}C]pyruvic acid (American Radiolabeled Chemicals, Inc.) and a large excess, 500 mM, of ManNAc in 50 mM potassium phosphate buffer, pH 7.4, for 24 h at room temperate. The lactate dehydrogenase (LDH) assay was used to confirm the complete consumption of pyruvic acid. An LDH stock solution (990 μL) of 5 mM $MgCl_2$, 0.1 mM KCl, 0.2 mM NADH, 10 U/mL LDH, in 50 mM Tris-OAc, pH 7.5, was measured at A_{340} until a stable absorbance was obtained. The reaction was initiated by addition of 10 μL of the NeuNAc aldolase reaction mixture. A decrease in A_{340} was indicative of residual pyruvic acid.

[1-^{14}C]NeuNAc was purified using a Mono-Q anion exchange column with a linear gradient of 1 to 80 mM ammonium acetate, pH 5.5, over 80 min and detected at A_{205} and A_{230}. [1-^{14}C]NeuNAc was collected, lyophilized, re-suspended in ddH_2O. Although the chemical yield of the unlabeled reaction was 100%, the labeled reaction resulted in a 3% chemical yield and 16% radioactive yield.

3.6 Synthesis of [1-^{14}C]NeuNAc oxime

Hydroxylamine-HCl (200 mM) was incubated with 10 mM [1-^{14}C]NeuNAc in ddH_2O for 7 h at room temperature. The [1-^{14}C]NeuNAc oxime was purified in the same way as [1-^{14}C]NeuNAc. The lyophilized product is re-suspended in 50 mM Tris-OAc, pH 8.3. The radioactive yield was 14%.

3.7 Synthesis of [1-^{14}C]PEP

Synthesis was carried out using phosphoenolpyruvate synthase (ppsA). ppsA expression and purification was previously reported.[49] [1-^{14}C]PEP was synthesized using 30 mM ATP, 12.5 mM [1-^{14}C]pyruvic acid, 20 mM $MgCl_2$, 1 mM dithiothreitol (DTT), and 10 mg/mL ppsA in 400 mM Tris-OAc, pH 8.4, at room temperature. After 10 min, the reaction was stopped by the addition of 210 mM NaOH and centrifuged at 13, 000 x g for 5 min. [1-^{14}C]PEP was purified using a Mono-Q column with a linear gradient of 0.1 – 1 M ammonium acetate, pH 5.5, over 100 min and detected at A_{240} and A_{280}. To reduce metal contamination, Chelex 100 was added to all purification buffers.

[1-^{14}C]PEP was collected, lyophilized, and re-suspended in 50 mM Tris-OAc, pH 8.3, and 1 mM EDTA. The Malachite Green assay was used to confirm that the purified PEP could be consumed by NeuB. [1-^{14}C]PEP was synthesized with chemical and radioactive yields of 56% and 34%, respectively.

3.8 Tracking NeuB inhibition with [1-^{14}C]PEP

NeuB (500 nM) was incubated with 2 mM ManNAc, 100 μM $MnCl_2$, 100 μM TCEP, 10 μM [1-^{14}C]PEP, and 63 mM NH_2OH in 50 mM Tris-OAc, pH 8.3, for 10 min at 37 °C. Following inhibition, a 0.5 mM PEP spike was added to the reaction mixture for better detection of the PEP peak at A_{240} and A_{280}. The reaction mixture was separated using a Mono-Q column with a 20 mM Tris-OAc, pH 8.5, wash buffer and a linear gradient of 0.01 – 1 M NaCl in 20 mM Tris-OAc, pH 8.5, over 80 min. Fractions were collected every 1 to 2 min until both [1-^{14}C]PEP and NeuB had eluted. Fractions were diluted 10-fold with Bio-Safe II scintillation cocktail (Research Products International Corp.) and analyzed using a liquid scintillation counter (1 min counting time) for radioactive counts per minute (cpm). Complete transfer of radioactivity from the PEP peak to the NeuNAc peak was indicative of control conditions where inhibition of NeuB did not occur. Inhibition was marked by decreased or halted reaction rates, leading to residual radioactivity in the PEP peak.

3.9 NeuNAc oxime inhibition during catalysis

Demetallated NeuB (250 nM) was incubated at 37°C with 15 mM ManNAc, 12 mM PEP, 2 mM $MnCl_2$, 100 μM TCEP, and 4 mM NeuNAc oxime in 50 mM Tris-OAc, pH 8.3. The extent of NeuB reaction in the presence and absence of inhibitor was assayed every 30 min for approximately 6 h. As the reaction proceeded and phosphate concentrations increased, aliquots at later time points were diluted with 50 mM Tris-OAc, pH 8.3, prior to mixing with Malachite Green reagent in order to keep phosphate in the measurable range.

In order to compare the difference between inhibition of catalyzing and non-catalyzing NeuB, reaction mixtures were pre-incubated with combinations of two out of the three substrate, PEP (12 mM), ManNAc (15 mM), and $MnCl_2$ (2 mM). Reaction mixtures containing two of the substrates, plus 4 mM NeuNAc oxime and 250 nM NeuB, in 50 mM Tris-OAc, pH 8.3, and 100 μM TCEP were pre-incubated at 37°C for 6 h. The reactions were started with the addition of the missing substrate and assayed at 37°C.

3.10 Data analysis

The k_{cat} and K_M values for PEP and ManNAc were fitted by non-linear regression to the Michaelis-Menten equation (Equation **2**).

$$v = \frac{V_{MAX}.[S]}{K_M + [S]} \quad (\mathbf{2}),$$

The dissociation constant, K_i, of the inhibitors was determined using the steady-state equation for competitive inhibition, with ordered binding of Mn^{2+} (A) and random binding of ManNAc (B) and PEP (C) (Equation **3**). The cooperativity of binding (α) between A and (B or C) was assumed to be 1.

$$\frac{v_0}{V_{MAX}} = \frac{\frac{[A][B][C]}{\alpha K_A K_B K_C}}{1 + \frac{[A]}{K_A} + \frac{[A][B]}{K_A K_B} + \frac{[A][C]}{K_A K_C} + \frac{[A][B][C]}{\alpha K_A K_B K_C} + \frac{[I]}{K_i}} \quad (\mathbf{3}),$$

where [A], [B], and [C] are substrate concentrations and K_A, K_B, and K_C are their respective K_M values. [I] is the inhibitor concentration and α = 1.

4 Results

4.1 NeuB substrate binding kinetics

The steady-state kinetic parameters for NeuB were determined in order to verify and compare enzyme behaviour with previous studies (Figure 15). The k_{cat} value was 2.63 ± 0.08 s^{-1} with K_M values for PEP and ManNAc of 121 ± 26 µM and 556 ± 141 µM, respectively.

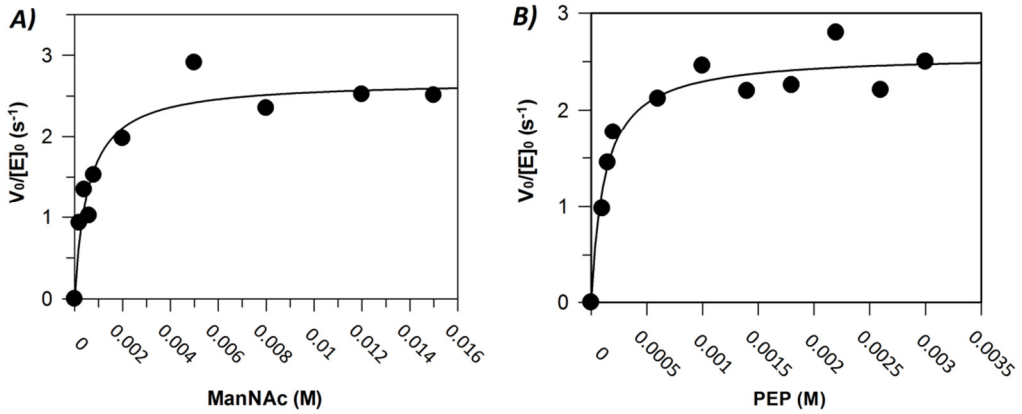

Figure 15. Steady state kinetic measurements for NeuB with A) ManNAc and B) PEP. The results show a V_{MAX} value of 2.6 (s^{-1}).

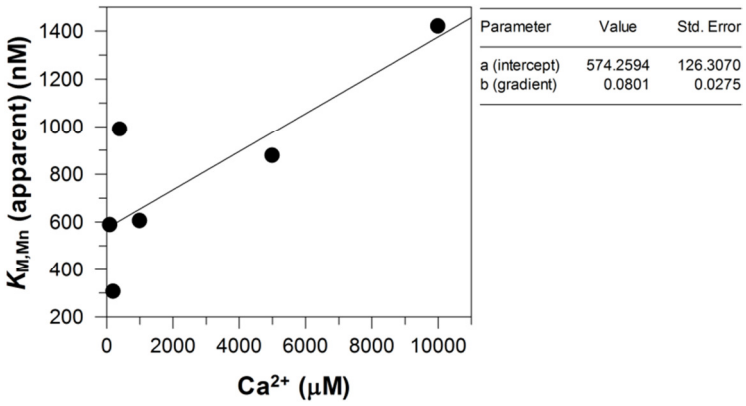

Figure 16. Relationship between $K_{M,Mn}$ and [Ca^{2+}]. Due to very tight binding between Mn^{2+} and NeuB, Ca^{2+} was used as a competitive inhibitor to remove Mn^{2+} from the active site. The y-intercept in this linear plot represents the true $K_{M,Mn}$, 574 ± 126 nM.

$K_{M,Mn}$ could not be determined using classic Michaelis-Menten kinetics, because NeuB co-purified with bound divalent cations, and was already active before exogenous Mn^{2+} was added. NeuB irreversibly lost activity if it was demetallated with EDTA and the EDTA was rigorously removed. Instead, NeuB was treated briefly with EDTA and desalted by gel filtration to remove the bulk of the EDTA. Ca^{2+}, which does not activate NeuB, was added to consume the remaining EDTA, then Mn^{2+} was added and reaction rates measured. A plot of Ca^{2+} concentration versus $K_{M,Mn}$ (apparent) shows that $K_{M,Mn}$ = 574 ±126 nM (Figure 16).

4.2 Synthesis and characterization of NeuB inhibitors

NeuNAc oxime and NeuNAc *O*-ethyl oxime were synthesized and characterized by ^{1}H-NMR and mass spectrometry as described previously.[47] (Adam Rosanally, Biochemistry 4B06 thesis).

NeuNAc *O*-fluoroethyl oxime was synthesized for the first time by allowing the reaction to progress for ~ 24 h, after which the inhibitor peak was fully formed (Figure 17). The peak corresponding to NeuNAc *O*-fluoroethyl oxime was purified and analyzed using mass spectrometry and ^{1}H-NMR (Figure 19). The average yield was ~ 75%. ^{19}F-NMR analysis of the inhibitor showed a peak at -224 ppm, confirming the presence of a single fluorine atom (Figure 18).

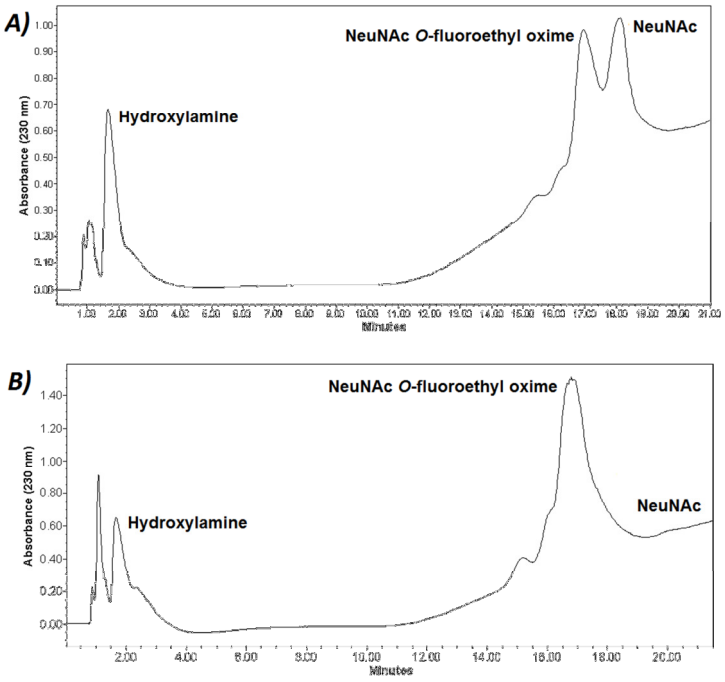

Figure 17. Tracking of NeuNAc *O*-fluoroethyl oxime synthesis at 230 nm on an anion exchange Mono-Q column following A) 10 min and B) 16 h.

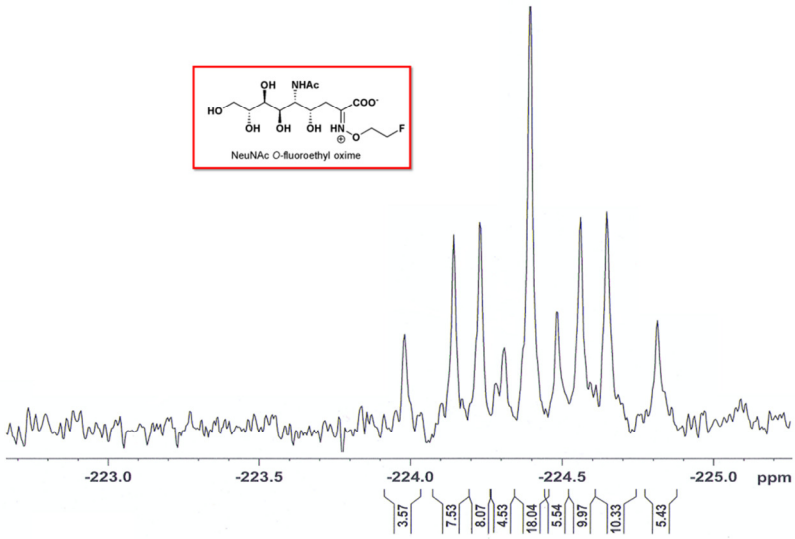

Figure 18. AV-200 MHz ^{19}F-NMR analysis of NeuNAc *O*-fluoroethyl oxime. A peak at -224 ppm confirms the presence of a single fluorine in the product. Peak splitting is due to neighboring ethyl protons.

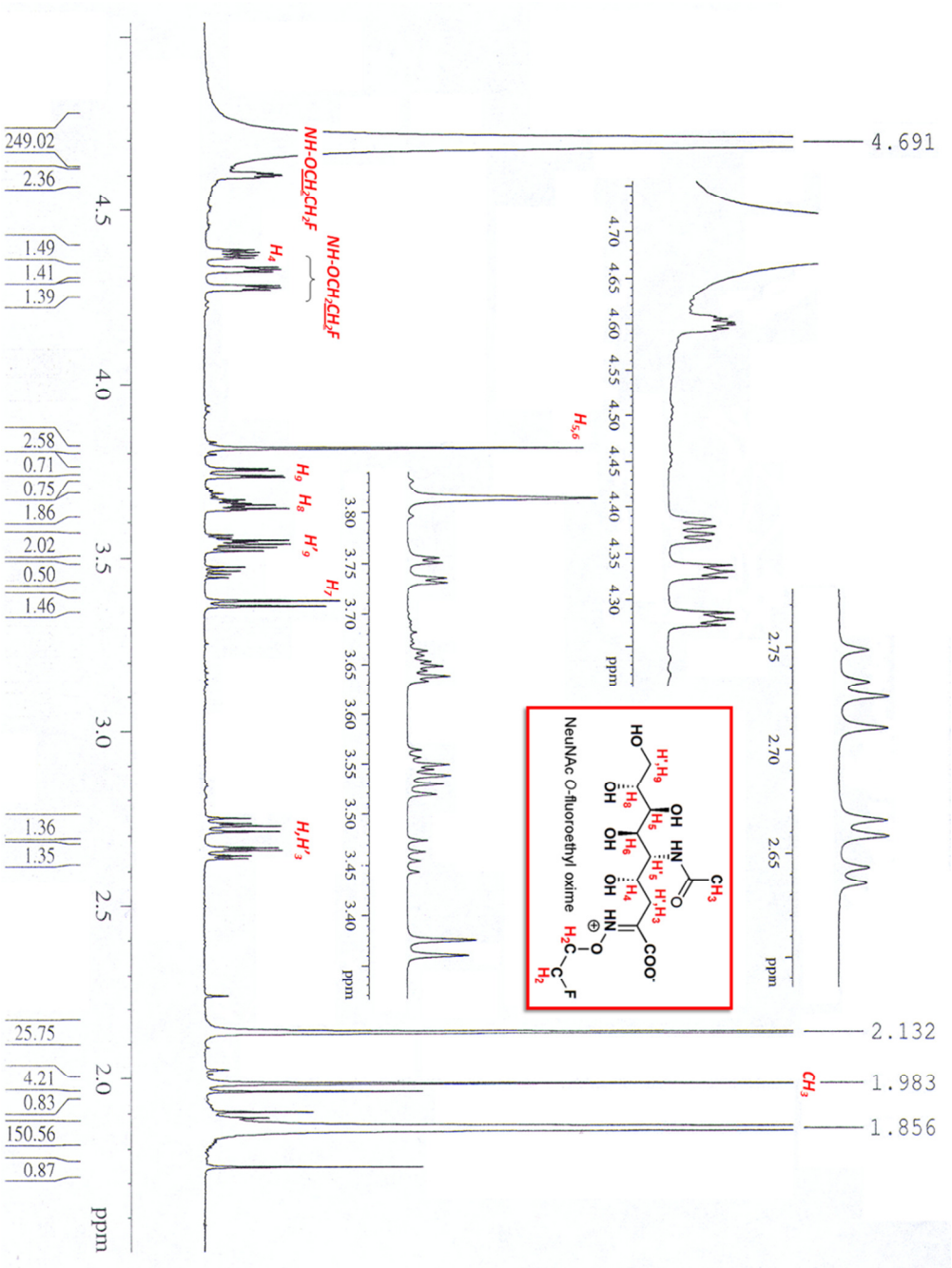

Figure 19. AV-600 MHz ^{1}H-NMR analysis of NeuNAc *O*-fluoroethyl oxime in D_2O. A 10 mM acetone peak is present at 2.1 ppm for quantification purposes.

4.3 Exploring inhibitory properties of NeuNAc oxime

NeuNAc oxime is a very tight binding inhibitor which gives incomplete inhibition (Figure 20). As with Edward Morrison's findings[47], we observed that NeuNAc oxime was unable to fully suppress NeuB activity – leaving 10% residual activity even with 117 μM inhibitor (data not shown) in our case, and 35% in his. The presence of residual activity, as opposed, for example, to adventitious PEP hydrolysis to release phosphate, was confirmed with HPLC-aided tracking of NeuNAc formation following inhibition (data not shown). The inhibition experiments were carried out by pre-incubating NeuB with NeuNAc oxime for 20 h at room temperature. The time-dependent inhibition was indicative of a slow-binding inhibitor. This was explored by tracking NeuB residual activity as a function of pre-incubation time with NeuNAc oxime (Figure 21). Assuming pseudo-first order rate kinetics, the rate of inhibitor binding (k_{on}) was 0.28 ± 0.08 h^{-1}, which corresponded to a half-life of binding of 2.5 h.

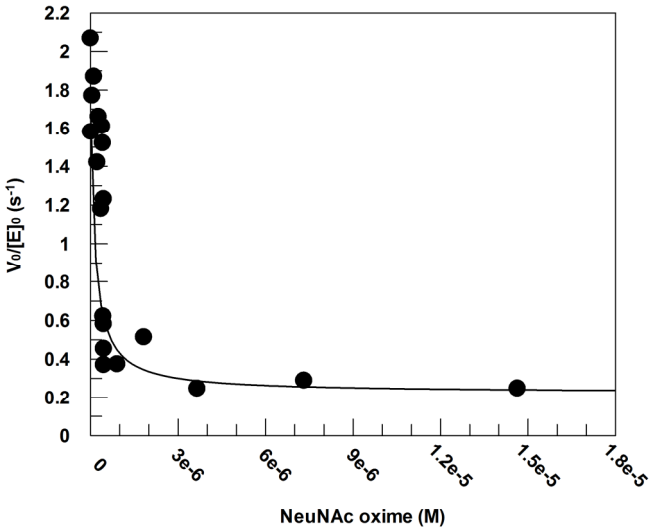

Figure 20. Inhibition profile of NeuNAc oxime with NeuB; fitted to equation 3. Reaction rates (s^{-1}) were determined with 0.91 mM Mn^{2+} and 1.8 mM ManNAc and PEP. A K_i value of 1.6(± 0.7) pM was observed.

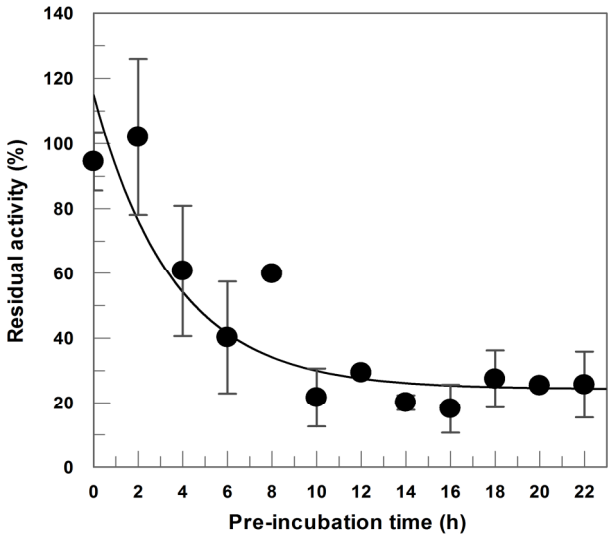

Figure 21. NeuNAc oxime binding as a function of pre-incubation time. NeuB residual activity decreased with increasing inhibitor pre-incubation time. The data was fitted to a single exponential decay equation with an offset of 24% residual activity.

4.4 The connection between NH_2OH and NeuNAc oxime inhibition

The mechanism for NH_2OH inhibition of NeuB is important for the further development and understanding of TS analogs for this enzyme. Previous evidence by Edward Morrison showed that NH_2OH inhibits NeuB by reacting with NeuNAc to create NeuNAc oxime; which is ultimately the inhibitory species.[47] Full inactivation of NeuB occurs following approximately 15 min and in the presence of 63 mM NH_2OH (Figure 22A). Interestingly, inhibition of NeuB in this manner is much quicker and does not result in residual activity. We verified these findings in this study (Figure 22B).

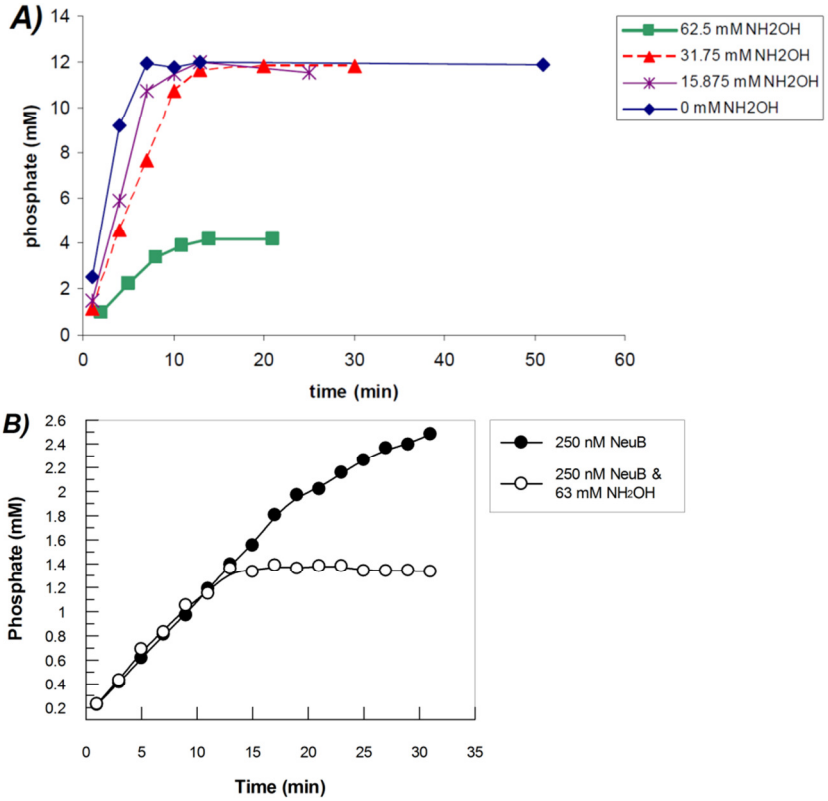

Figure 22. Inhibition of NeuB by NH_2OH in the presence of substrates is complete and time-dependent. A) Previous concentration dependence tests showed that 63 mM NH_2OH is required for full inhibition of NeuB (From reference [47]). B) We verified these findings in this study.

The overall progress curve is consistent with that of a slow-binding inhibitor; though a rapid onset of inhibition is observed at approximately 15 min. This suggests that the production of a certain quantity of NeuNAc is required for inhibition. However, we have observed variability in the amount of NeuNAc formed as well as the time required for inhibition. Since enzyme activity is the only component of the assay susceptible to fluctuation, we believe that it is responsible for this variability. NH_2OH inhibition studies suggest that NeuNAc oxime has the potential to be a powerful inhibitor and that it is possible to resolve the issues associated with very slow-binding and residual activity.

4.5 Binding of [1-^{14}C]NeuNAc oxime to NeuB

Synthesis and purification of [1-^{14}C]NeuNAc, and subsequently [1-^{14}C]NeuNAc oxime, was performed in hope of directly demonstrating that inhibited NeuB was complexed with NeuNAc oxime. Given the difference in behaviours between NH_2OH, which gave relatively rapid and complete inhibition, and NeuNAc oxime, which had high affinity, but slow onset inhibition, and residual activity at high inhibitor concentrations, the concern was that NH_2OH inhibition was occuring through some mechanism other than NeuNAc oxime formation. However, low chemical and radioactive yields prevented us from synthesizing an adequate quantity of pure [1-^{14}C]NeuNAc oxime. The final radioactive yield of [1-^{14}C]NeuNAc oxime from [1-^{14}C]pyruvic acid was only 0.36%. Also, maximal NeuB inhibition requires pre-incubation of 5 μM enzyme with 122 μM NeuNAc oxime. This is problematic because, upon enzyme-inhibitor binding, the

resulting theoretical peak associated with NeuB radioactivity will not exceed 4% of the NeuNAc oxime peak.

4.6 Tracking NeuB inhibition with [1-^{14}C]PEP

Tracking the radioactive signal associated with [1-^{14}C]PEP consumption was used to elucidate NeuB inhibition in the presence of NH_2OH. This experiment was carried out in order to definitively show weather NeuNAc oxime was the inhibitory agent during NH_2OH inactivation of NeuB. If true, the experiment presented an alternative route for showing direct binding of NeuNAc oxime to NeuB. Unfortunately, the transfer of radioactivity from [1-^{14}C]PEP to NeuNAc, and eventually the NeuB•NeuNAc oxime complex, was not observed. We showed that in the absence of NH_2OH, 500 nM NeuB consumed 84% of 50 μM [1-^{14}C]PEP in 10 min, but with 63 mM NH_2OH, only 8% of [1-^{14}C]PEP was consumed (Figure 23 and 24).

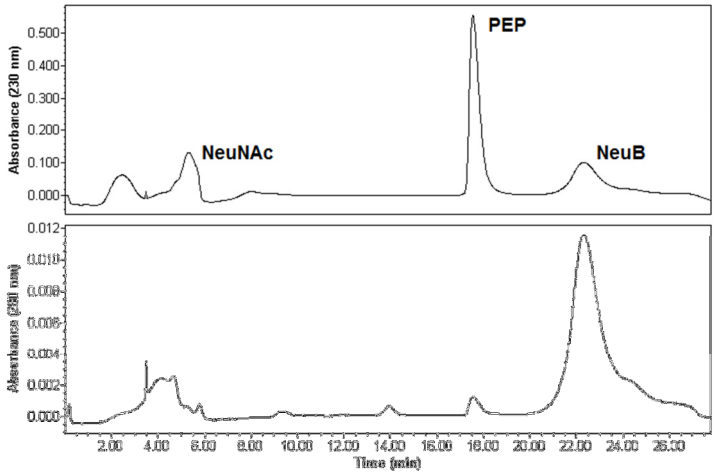

Figure 23. Elution of NeuNAc, PEP and NeuB on an anion exchange Mono-Q column with a linear gradient of 0.1 – 1 M NaCl in 20 mM Tris-OAc, pH 8.5, and detection at A_{230} and A_{280}.

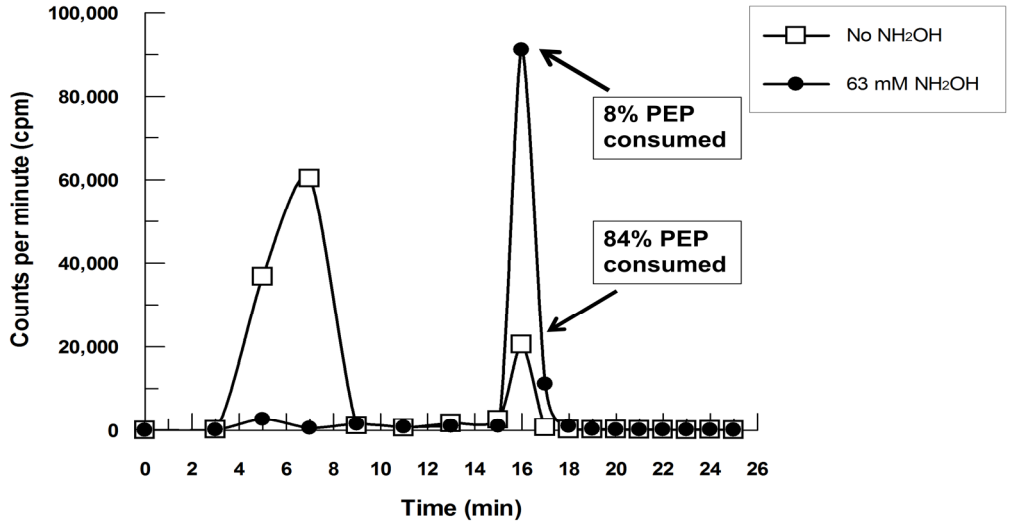

Figure 24. Radioactivity trace of 10 min 500 nM NeuB reactions with 50 μM [1-^{14}C]PEP in the presence and absence of 63 mM NH_2OH. NeuB consumed 84% of PEP in the absence of NH_2OH, while only 8% was consumed in the presence of 63 mM NH_2OH.

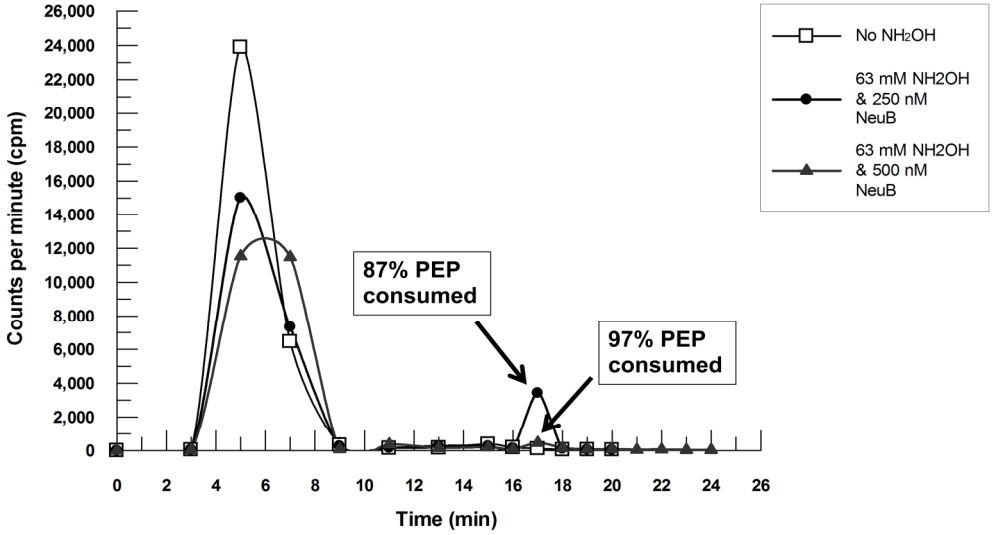

Figure 25. Radioactivity trace of 10 min 250 and 500 nM NeuB reactions with 10 μM [1-^{14}C]PEP in the presence and absence of 63 mM NH_2OH. NeuB consumed 100% of PEP in the absence of NH_2OH. In the presence of 63 mM NH_2OH, 97% of PEP was consumed with 20-fold excess of PEP to NeuB, and 87% of PEP was consumed with 40-fold excess of PEP to NeuB.

Inhibition is visible under these conditions and the signal associated with the proposed NeuB•[1-^{14}C]NeuNAc oxime complex would theoretically reach ~ 1,000 cpm. This signal would be expected during NeuB elution at 18 – 22 min (Figure 24). However, no radioactivity is visible in this region. Optimization of these conditions showed that inhibition can still occur with 250 nM and 500 nM NeuB with 10 μM [1-^{14}C]PEP (Figure 25). Using 250 nM NeuB and 10 μM [1-^{14}C]PEP (51 nCi), the radioactivity associated with the NeuB•[1-^{14}C]NeuNAc oxime complex was expected to reach ~ 3,000 cpm. This is well above the baseline in the region corresponding to NeuB elution (20 – 24 min). However, no elevation in radioactivity was visible in this region either. The experiment with 500 nM NeuB and 10 μM [1-^{14}C]PEP showed that 20-fold excess of PEP to NeuB is the lower limit required for inhibition. In this case, 97% of the PEP was broken down prior to inhibition.

4.7 NeuNAc oxime inhibition during catalysis

NeuNAc oxime showed complete inhibition of NeuB when incubated with substrates over 6 h (Figure 26). With 250 nM NeuB and 4 mM NeuNAc oxime, enzyme activity began to decrease following the 2 h mark. The control data was non-linear due to time-dependent loss of enzyme activity and/or substrate consumption. Therefore, the results are fitted to a first order rate equation which shows the rate of inactivation (k_{inact}) for inhibited and uninhibited NeuB during catalysis.

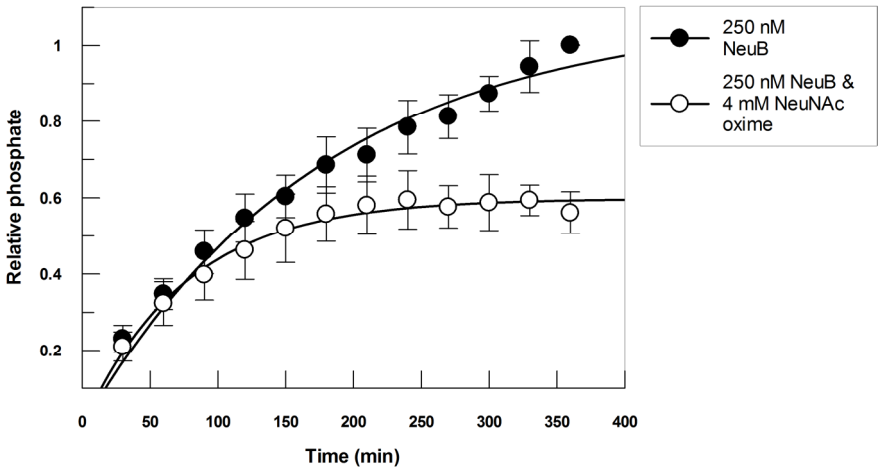

Figure 26. The rate of NeuB inactivation in the presence and absence of NeuNAc oxime over 6 h. Phosphate values were normalized to account for variability in enzyme activity.

The rate of activity loss for inhibited and uninhibited NeuB was k_{inact} = 0.0132 ± 0.0007 min^{-1} and 0.0057 ± 0.0006 min^{-1}, respectively. The rate of NeuB inactivation was increased 2.3-fold in the presence of NeuNAc oxime. This trend is comparable to the previously observed time-dependent NH_2OH inactivation of NeuB (Figure 22).[47] This suggests that inhibition of catalyzing NeuB by NH_2OH and exogenous NeuNAc oxime follows a similar mechanism.

To illustrate the difference between inhibition of catalyzing and non-catalyzing NeuB, NeuB and NeuNAc oxime were pre-incubated with two of the three substrates for 6 h at 37°C. The third substrate was used to start the reaction following the pre-incubation. We observed that NeuNAc oxime was unable to fully inhibit NeuB when pre-incubated with ManNAc and Mn^{2+}, PEP and Mn^{2+}, or ManNAc and PEP (Table 1). Further, we observed a noticeable change in inhibition depending on which combination of substrates NeuNAc oxime was pre-incubated with. The most potent inhibition

occurred in the presence of ManNAc and Mn^{2+}, followed by PEP and Mn^{2+}. In the case of ManNAc and PEP, no inhibition was observed.

Table 1. Extent of NeuB inhibition by NeuNAc oxime when pre-incubated with two of its substrates at 37°C for 6 h.

Pre-incubating substrates	Rate in the absence of NeuNAc oxime (s^{-1})	Rate in the presence of NeuNA oxime (s^{-1})	Residual activity (%)
ManNAc and Mn^{2+}	1.8	0.7	39
PEP and Mn^{2+}	1.8	1.1	59
ManNAc and PEP	2.2	2.8	128

5 Discussion

5.1 NeuB substrate binding kinetics

The correct substrate K_M values are essential for characterizing enzyme inhibition because K_i is a function of both K_M and [S] for each substrate. Table 2 shows the previously reported K_M values for NeuB at pH 8.3.

Table 2. Previously reported K_M and k_{cat} values for NeuB at pH 8.3 in comparison with our findings.

Reference	$K_{M,ManNAc}$	$K_{M,PEP}$	$K_{M,Mn}$	k_{cat} (s^{-1})
Morrison, E.[47]	3.7 mM	580 μM	59 μM	1.6
Gunawan *et al.*[21]	9.4 mM	250 μM	-	0.9
Blacklow *et al.*[50]	6.3 mM	40 μM	-	-
This work	556 μM	121 μM	574 nM	2.63

The previously reported $K_{M,ManNAc}$ values fall in the low millimolar range and are generally higher than our value of 556 μM. Our $K_{M,PEP}$ value of 121 μM is similar to previously reported values, which are all in the micromolar range. The slight discrepancy between these values is most likely due to differences in assay conditions. Studies by Gunawan *et al.* and Blacklow *et al.* were conducted in 150 mM Tris-OAc; whereas our studies, including those of Morrison, E., were conducted in 50 mM Tris-OAc. Further, our reducing agent in the assay was TCEP instead of DTT. Under these conditions, we also report a relatively higher k_{cat} value of 2.6 s^{-1}. The increased k_{cat} value is attributed to the use of demetallated enzyme in the assay. It was likely that demetallation of purified NeuB increases reaction rates by removing metals which were co-purified with the

enzyme and were less activating than Mn^{2+}. It has been shown that *in vitro* NeuB activation by Ca^{2+}, Ni^{2+}, Fe^{2+}, and Ba^{2+} is very low compared to Mn^{2+} (Table 3).[20] DAH7P synthase is also co-purified with a variety of metals and shows similarly high *in vitro* activation by Mn^{2+}.[51] However, the true *in vivo* metal for DAH7P synthase is likely Fe^{2+} or Zn^{2+}, based on their presence in purified enzymes and their high bioavailability.[51]

Table 3. Relative *in vitro* NeuB activation by various divalent metal co-factors. From reference [20].

Metal ion	Relative activity (%)*
Co^{2+}	235
Mg^{2+}	86
Cd^{2+}	17
Zn^{2+}	15.2
Ni^{2+}	14
Fe^{2+}	4.6
Ba^{2+}	0.63
Ca^{2+}	0.61

* Relative to Mn^{2+}

Determining $K_{M,Mn}$ was complicated by NeuB's high affinity for metal ions. Purified NeuB was slightly active due to contaminating metals prior to Mn^{2+} addition. We were successful in removing these metals with 1 mM EDTA. However, gel filtration was unsuccessful at fully separating NeuB from residual EDTA. In cases where EDTA was rigorously removed by dialysis, NeuB was irreversibly inactivated. Therefore, we determined $K_{M,Mn}$ by using Ca^{2+} to chelate EDTA. Ca^{2+} was used to i) bind residual EDTA and ii) act as a competitive inhibitor for Mn^{2+}. $K_{M,Mn}$ (apparent) increased with

increasing Ca^{2+}, showing that the metal ions were binding competitively with NeuB. The y-intercept gave the true $K_{M,Mn}$ value, 574 nM. To our knowledge, this is the first report of an accurate $K_{M,Mn}$ value for NeuB. This value was lower than obtained in cases where competing metals were not as rigorously excluded. Edward Morrison reported a $K_{M,Mn}$ value of 59 ± 19 μM under such conditions.[47]

The common feature between all reported substrate binding constants is that the lowest value is associated with the metal co-factor, followed by PEP and ManNAc. This trend has also been observed with DAH7P (Naresh Balachandran, personal communication) and KDO8P synthases.[52] Previous evidence with DAH7P and KDO8P synthase has also shown ordered substrate binding, with PEP binding prior to the aldose.[52-53] The initial binding of the metal co-factor is assumed given its low K_M and deep placement in the active site. It is possible that similar ordered substrate binding also occurs with NeuB.

5.2 NeuNAc oxime inhibition kinetics

We have confirmed that pre-incubation of NeuB and NeuNAc oxime together is essential for obtaining maximal inhibition. This was first observed in Edward Morrison's work.[47] Similar trends have also been reported with oxacarbenium mimic inhibitors for KDO8P and DAH7P synthases.[18,43-46] Prior to our kinetic studies with NeuNAc oxime, we were able to optimize assay conditions in order to increase the potency of the inhibitor. Inhibition was improved by excluding BSA from the assay and pre-incubating

NeuB and NeuNAc oxime for 20 h at 25°C. BSA is often used in assays in order to stabilize enzymes and increase reaction rates. However, its sponge-like ability to bind a wide array of ligands can sometimes affect inhibition assays by non-specifically binding the inhibitor.

Kinetic studies under these conditions showed that NeuNAc oxime inhibited NeuB with an apparent K_i value of 1.6 pM and a half-life for binding of 2.5 h. Having measured the K_i and k_{on}, we calculated the k_{off} to be 3.2×10^{-11} s^{-1}, or $t_{1/2} = 2.1 \times 10^{10}$ h. This data shows that NeuNAc oxime is a slow-binding inhibitor, which is characteristic of most TS analogs. The slow-binding suggests that the formation, or further conformational adjustment, of the NeuB•NeuNAc oxime complex is slower than the overall reaction rate. Previous studies have attributed slow-binding kinetics to domain movements that accompany inhibitor binding.[54-55] In the case of NeuB, we know that large movements are involved in catalysis, primarily of the type III antifreeze domain. This domain occludes the NeuB active site in the crystal structure, and contributes a residue, Arg314, to the active site of the opposing subunit of the monomer. We can postulate that anything hindering or not inducing the proper movement of this domain will cause slow-binding of substrates or inhibitors. During normal catalysis, enzyme substrates and products are able to induce conformational changes which ensure the proper and timely binding and release of these ligands. One example is the complex choreography of enolpyruvyl UDP-GlcNAc (MurA) product release.[56] The release of phosphate from MurA is mediated by Arg397 as it rotates and tracks the bound phosphate from the enzyme active site into

solution. Therefore, it is possible that NeuNAc oxime is not able to induce the proper conformational change in NeuB required for quick and efficient binding. Others have shown that the conformational adjustment made by inhibitors in order to chelate the active site metal is responsible for time-dependent inhbition.[57]

Although the ultimate affinity of NeuNAc oxime is high, there is NeuB residual activity (~ 10%) following inhibition. This trend was observed with other α-carboxyketose synthases such as DAH7P synthase (Naresh Balachandran, personal communication) and the THI mimic of NeuB[26] (Martin Tanner, personal communication). The extent of residual activity can vary between 10 – 50%. It is still not fully clear what causes this incomplete inhibition or its fluctuation. We suspect that certain differences in inhibitor and enzyme batches can influence the extent of inhibition. This issue is discussed in more detail below.

5.3 Tracking NeuB inhibition with [1-^{14}C]PEP

We originally attempted to show direct binding between NeuNAc oxime and NeuB by synthesizing [1-^{14}C]NeuNAc oxime. However, given NeuB's activity loss upon overnight incubation, combined with significant problems with the yield of radiolabelled inhibitor, trapping [1-^{14}C]NeuNAc oxime directly with NeuB was not possible. Instead, trapping was attempted using [1-^{14}C]PEP and NH_2OH to form the inhibitor *in situ*. We would expect that enzymatic formation of [1-^{14}C]NeuNAc, followed by spontaneous [1-^{14}C]NeuNAc oxime formation, either in the NeuB active site or in solution, would

inhibit the enzyme. Although we observed inhibition of NeuB, we were unable to detect the transfer of radioactivity from PEP to the NeuB•[1-^{14}C]NeuNAc oxime complex. One reason for this is that time-dependent NH_2OH inhibition required excess substrates. That is, good inhibition was not observed unless we used a 40-fold excess of PEP to NeuB. The need for excess substrates meant that it was not possible to observe inhibition with equimolar NeuB and [1-^{14}C]PEP. Given the required excess of PEP, only a small fraction of the radioactive label associated with [1-^{14}C]PEP would be transferred to the NeuB•[1-^{14}C]NeuNAc oxime complex. With 40-fold excess of [1-^{14}C]PEP to NeuB, only 3% of the radioactive label was expected to be transferred to the NeuB•[1-^{14}C]NeuNAc oxime complex. The low signal transfer most likely contributed to our inability to detect radioactive label in this proposed complex. It is also possible that the NeuB•[1-^{14}C]NeuNAc oxime complex did form, but were separated during the Mono-Q purification step, as it is possible or likely that the initially formed complex is not as tightly bound as the E^*•I complex formed after overnight incubation.

Despite not achieving our initial goal, the study with [1-^{14}C]PEP and NH_2OH did provide insight into the inhibition mechanism of NH_2OH. We were able to show that inhibition was achieved more quickly in the presence of larger excesses of PEP. For example, in the presence of 100-fold excess of PEP, only 8 mol was consumed per mol of NeuB prior to reaction inhibition; whereas with 40-fold excess of PEP, 35 mol was consumed per mol of NeuB (Figure 24 and 25). Since all experimental PEP concentrations were below $K_{M,PEP}$, it follows that PEP concentrations influenced the

reaction rate. These results seemed to suggest a connection between NH_2OH inhibition and catalysis. Reactions in which NeuB was turning over quickly appeared to be much more susceptible to inhibition than slower catalysis. Also, if such catalysis was not sustained for long enough, as was the case with 20-fold excess of PEP, the reaction was not susceptible to inhibition. Inhibition with 20-fold excess of PEP occurred following the breakdown of 97% of PEP; suggesting that this was the lower limit for excess substrates required for inhibition.

Thus we proposed the existence of two important NeuB conformational states, idle state NeuB ($NeuB^{IS}$) and running state NeuB ($NeuB^{RS}$). $NeuB^{IS}$ is characterized by slow NeuNAc oxime binding and incomplete inhibition. The latter is most likely the result of binding to only one monomer of the dimer. There is evidence that the unbound monomer has a lower k_{cat}, otherwise the residual activity would be 50%. $NeuB^{RS}$ is characterized by faster NeuNAc oxime binding and complete inhibition. In this case, the latter could be due to inhibitor binding to both monomers or to one monomer, with a concomitant conformational change that inactivates the second monomer. Excess substrates are responsible for maintaining high and sustained concentrations of $NeuB^{RS}$ needed to drive the binding reaction with the *in situ* generated NeuNAc oxime. Further, excess substrates ensure that a sufficient concentration of NeuNAc oxime is produced in order to elicit inhibition. Figure 27 illustrates two possible mechanisms for NH_2OH inhibition. NH_2OH can react with NeuNAc directly in the active site or once it has been released into solution in order to form NeuNAc oxime.

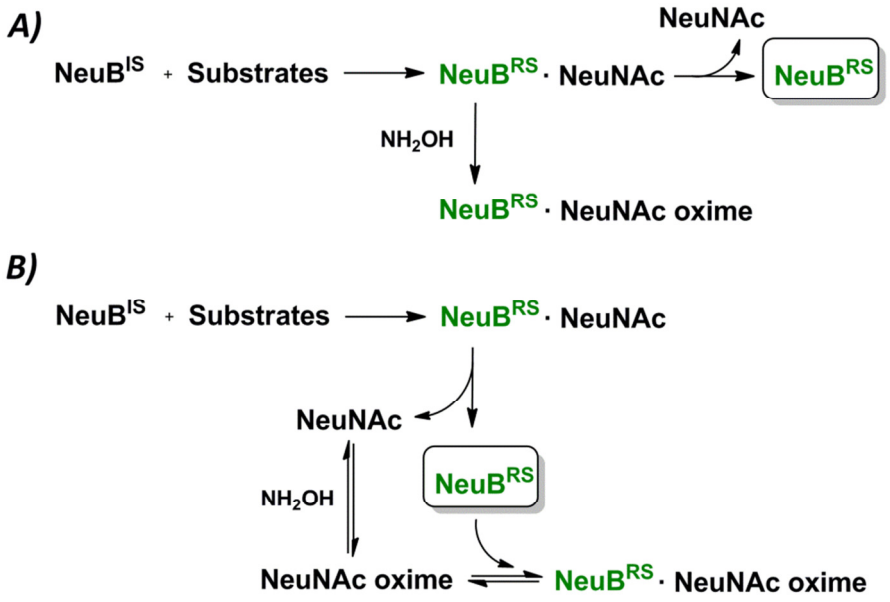

Figure 27. Two proposed mechanisms of NeuB inhibition in the presence of substrates and NH_2OH. A) NH_2OH reacts with NeuNAc directly in the active site of NeuB, forming NeuNAc oxime. B) NeuNAc is released and reacts with NH_2OH in solution. The formed NeuNAc oxime will bind free $NeuB^{RS}$. High and sustained concentrations of $NeuB^{RS}$ make complete inhibition of NeuB possible.

If correct, this hypothesis would further our understanding of the inhibition mechanism for NeuB and possibly other α-carboxyketose synthases. It suggests that NeuNAc oxime inhibition is more potent when NeuB is performing catalysis and therefore generating $NeuB^{RS}$. Further, it explains how enzyme activity might be associated with NeuNAc oxime inhibition. Less active NeuB will not be able to generate high and sustained concentrations of $NeuB^{RS}$, resulting in slower and possibly less potent inhibition. This is similar to what we have observed with excess substrates.

5.4 NeuNAc oxime inhibition during catalysis

In an effort to validate the proposed NH_2OH inhibition mechanism, we sought to directly inhibit catalyzing NeuB with extrinsically synthesized NeuNAc oxime. All previous NeuNAc oxime inhibition experiments had involved the pre-incubation of enzyme and inhibitor only. The incubation of NeuB and its substrates with NeuNAc oxime over an extended period illustrated the difference in inhibition of catalyzing and non-catalyzing enzyme. Our results indicated that catalyzing NeuB can be completely inhibited by NeuNAc oxime over 6 h at 37°C. As with NH_2OH inhibition, the progress curve showed an initial reaction burst followed by a slow steady-state rate, confirming that NeuNAc oxime is a slow-binding inhibitor. The inhibition was considerably slower than previously observed with NH_2OH, but faster than with non-catalyzing NeuB. More importantly, this was the first observed case of complete inhibition by NeuNAc oxime. In order to further distinguish inhibition of catalyzing and non-catalyzing NeuB, we attempted to inhibit the enzyme by pre-incubating it with two of its substrates and the inhibitor for 6 h at 37°C. We observed that no combination of two substrates could promote complete inhibition of non-catalyzing NeuB. This shows strong evidence for the idea that actively catalyzing NeuB is more effectively inhibited by NeuNAc oxime than non-catalyzing NeuB. We propose that the mechanisms of NeuB inhibition by exogenous and *in situ* generated NeuNAc oxime are similar (Figure 28). As with NH_2OH inhibition, faster reaction rates will promote high and sustained concentrations of $NeuB^{RS}$ required for potent inhibition.

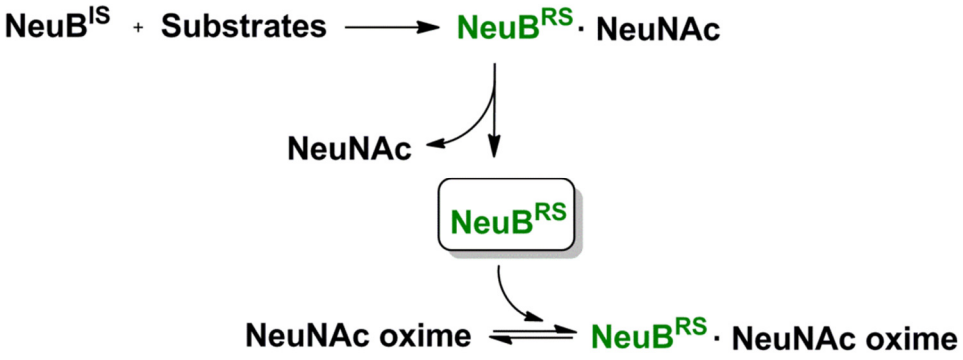

Figure 28. NeuB inhibition mechanism by NeuNAc oxime in the presence of substrates. NeuNAc oxime binds favorably to free $NeuB^{RS}$ following release of NeuNAc.

The binding of ligands to specific conformational states during enzyme catalysis is a commonly accepted phenomenon.[58-59] The dynamic nature of enzymes means that they exist in a number of different microstates; which can arise as a result of catalysis or simply due to isomerization of the free enzyme in solution. Ligands (i.e., substrates, products, intermediates, or inhibitors) will bind preferentially to one microstate or subset of microstates depending on the structural complementarily between the ligand and the binding pocket of that microstate.[58] If the binding is very favorable, the ligand will stabilize the microstate and trap the enzyme in this particular conformation.[59] Therefore, it is possible that $NeuB^{RS}$ is a preferred microstate for NeuNAc oxime.

Finally, it should be noted that the slow onset of inhibition suggests that inhibitor binding to the active site is a rare occurrence. By the time complete inhibition has occurred, each molecule of enzyme has turned over ~ 40,000 reactions.

5.5 Residual activity

We have determined that residual activity is associated with binding of NeuNAc oxime to non-catalyzing NeuB. Inhibition of catalyzing NeuB with NH_2OH or exogenous NeuNAc oxime leads to complete inhibition. We have also observed that residual activity is variable between 10 – 50%. Dadi *et al.* observed similar residual activity in their attempt to inhibit ATPase with various polyphenols.[60] However, they were unable to determine its cause. Interestingly, they did not report inhibition of catalyzing ATPase, but rather with the pre-incubation of only enzyme and inhibitor. The NeuB THI mimic inhibitor (Section 1.6, compound **8)** was also shown to exhibit residual activity following a 20 min pre-incubation (Martin Tanner, personal communication). Likewise, inhibition of DAH7P synthase by DAH7P oxime shows 25% residual activity following a 40 min pre-incubation (Naresh Balachandran, personal communication).

Increasing evidence suggests that residual activity may be linked to slow-binding inhibitors which follow a two-step isomerization mechanism.[61-64] Residual activity following enzyme inhibition by a slow-binding inhibitor can be related to the equilibrium between E•I and E^*•I (Figure 29). In situations where k_{-2} is a nonzero value such that an appreciable percentage of E•I exists following the pre-incubation of enzyme and inhibitor, this percentage will equal the observed residual rate (Equation **4**).

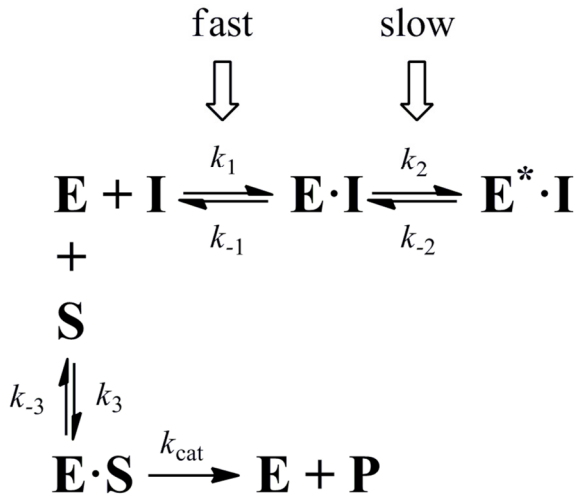

Figure 29. Slow-binding inhibitors which follow a two-step isomerization mechanism can produce residual activity following pre-incubation of enzyme and inhibitor due to the equilibrium between E•I and E*•I. The percentage of total enzyme existing in the E•I complex at equilibrium corresponds to the observed residual activity.

Since E•I is always in rapid equilibrium with free enzyme, the final percentage of enzyme existing in this complex can be rapidly shifted towards E•S formation in the presence of excess substrates. This does not occur with the E*•I complex because, even with excess substrates, formation of E•S is limited by the slow rate of k_{-2}. This hypothesis offers a sound argument for the source of residual activity associated with slow-binding inhibitors, such as NeuNAc oxime.

$$\%\mathrm{E}^{*}\bullet\mathrm{I}_{sat} = \frac{k_2}{k_2 + k_{-2}} \times 100 \qquad \textbf{(4)},$$

where $\%E^{*}\bullet I_{sat}$ is the percentage of total enzyme existing in the E*•I complex following pre-incubation and k_2 and k_{-2} are the rates of formation and breakdown of E*•I, respectively.

Further, crystallography studies with DAH7P synthase have shown that the oxime inhibitor binds to only two of its four subunits (Naresh Balachandran, personal communication). It is also plausible that in solution, NeuNAc oxime binds to only one of its two subunits – leaving the other partially active. Such a scenario would be consistent with partial inhibition. A partial inhibitor is one which leaves the E•I complex partially active; this allows for subsequent binding and turnover of substrates by this complex.[59] During catalysis, unknown conditions arise that allow the inhibitor to occupy both active sites or fully eliminate the activity of the unoccupied site. It is also important to note that non-catalyzing DAH7P synthase can be completely inhibited with DAH7P *O*-fluoroethyl oxime (Naresh Balachandran, personal communication). This suggests that residual activity is a reflection of the specific enzyme-inhibitor combinations, not solely of the enzyme.

6 Conclusion and future work

We have explored the inhibition of NeuB by an oxacarbenium mimic inhibitor, NeuNAc oxime, and shown it to be a slow-binding inhibitor. When pre-incubated with enzyme and assayed for inhibition, NeuNAc oxime has shown tight-binding (K_i^* = 1.6(± 0.7) pM) that left a residual enzyme rate between 10% and 50% with k_{on} = 0.28 ± 0.08 h^{-1} and a half-life for binding of 2.5 h. Interestingly, inhibition of substrate catalyzing NeuB over 6 h with NeuNAc oxime showed faster and complete inhibition. This is similar to the previously observed time-dependent inactivation of NeuB by NH_2OH; which occurs as a result of *in situ* generation of NeuNAc oxime when NH_2OH reacts with the NeuB product, NeuNAc. We have made a distinction between inhibition of actively catalyzing and non-catalyzing NeuB. We postulate that this is caused by weak binding between NeuNAc oxime and $NeuB^{IS}$, as opposed to $NeuB^{RS}$ which is generated during enzyme catalysis.

Future work should be directed towards fully resolving the kinetic properties of the NeuNAc *O*-ethyl and *O*-fluoroethyl oxime inhibitors (i.e., K_i, k_{on}). Do these inhibitors show similar potency with catalyzing and non-catalyzing NeuB? A second attempt could be made to trap radiolabeled NeuNAc oxime with NeuB. Excess labeled inhibitor did not allow us to transfer a significant percentage of radioactivity to NeuB. Therefore, dialysis following inhibition could be performed in order to remove excess radioactivity associated with unbound inhibitor. Also, one unexplored area which appears important

for catalysis and inhibition is the antifreeze-like domain. In order to study the role of this domain, we propose to track its movement during catalysis using transition metal ion fluorescence resonance energy transfer (FRET).[65-66] This technique offers advantages over classical FRET because it uses small probes with short linkers in order to measure short-range distances in proteins. Classical FRET employs large probes (15 – 30 Å) with long, flexible linkers (10 – 15 Å) which detect distances in the 30 – 60 Å range. Therefore, this technique is not practical for detection of intramolecular protein movements. Transition metal ion FRET uses a small fluorescence donor, monobromobimane (mBBr), which is comparable in size to a natural amino acid, and three transition metal ion acceptors, Ni^{2+}, Cu^{2+}, and Co^{2+}.[66] mBBr is a thiol-reactive probe which can be directly attached to any surface exposed cysteine residue. Similarly, the metal ions can be attached to dihistidine sites or small cysteine-attached metal chelators such as nitrilotriacetic acid (NTA), EDTA, and iminodiacetic acid (IDA). The advantage of this technique is that FRET is limited to the 5 – 20 Å range.[66] If the antifreeze-like domain is responsible for capping the NeuB active site, we should observe its movement as it opens and closes the active site. Mutagenesis experiments are required to generate two ideally spaced and surface exposed cysteine residues, which will anchor FRET donor and acceptor molecules. One molecule will be positioned close to the *C*-terminal end of the antifreeze-like domain, while the second will be on the TIM barrel such that it is in close proximity to the first molecule upon closing of the active site. This will ensure that the FRET signal is only transferred upon closing of the active site. Fortunately, the only wild type NeuB surface exposed cysteine residue, Cys249, is on the

C-terminal end of the antifreeze-like domain. Therefore, it is likely that only one cysteine mutation has to be made; Glu66 and Gln69 are two promising targets as they are in close proximity to Cys249 (Figure 30). Attachment of a metal chelator to one of these two sites will place the metal ion acceptor either 14 Å or 21 Å away from mBBr. It is essential the enzyme activity is retained upon addition of the FRET probes.

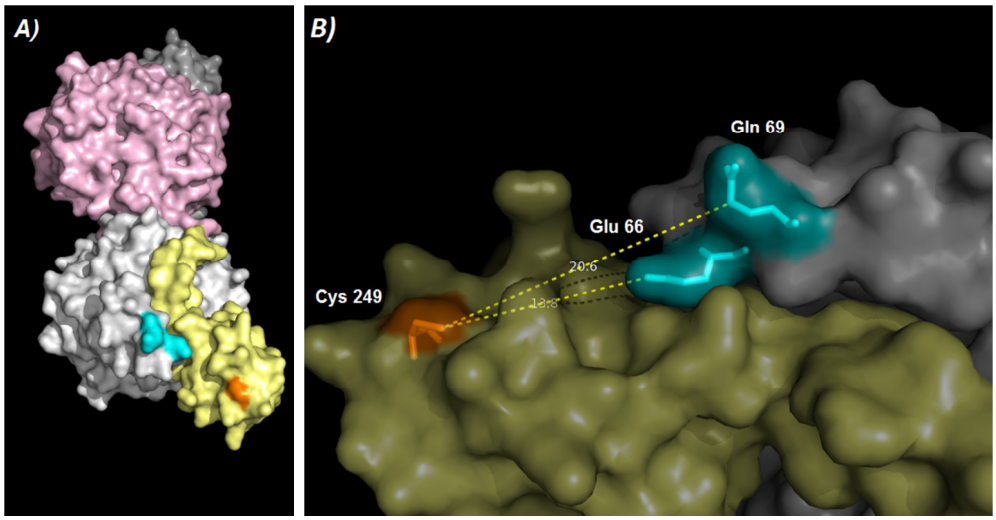

Figure 30. Strategy for introducing a thiol-reactive FRET pair to detect movement of the NeuB antifreeze-like domain. A) Cys249 (orange) is a wild type surface exposed cysteine which resides on the *C*-terminal end of the antifreeze-like domain (yellow). B) A second surface exposed cysteine must be generated by mutation of either Glu66 or Gln69 (blue).

7 References

(1) Traving, C.; Schauer, R. *Cell. Mol. Life Sci.* **1998**, *54*, 1330-1349.

(2) Schauer, R. *Glycoconj. J.* **2000**, *17*, 485-99.

(3) Schauer, R. *Trends Biochem. Sci.* **1985**, *10*, 357-360.

(4) Pilatte, Y.; Bignon, J.; Lambré, C. R. *Glycobiology* **1993**, *3*, 201-218.

(5) Varki, A. *Glycobiology* **1992**, *2*, 25-40.

(6) Durocher, J. R.; Payne, R. C.; Conrad, M. E. *Blood* **1975**, *45*, 11-20.

(7) Schauer, R. *Arch. Biochem. Biophys.* **2004**, *426*, 132-41.

(8) Stephens, D. S.; Greenwood, B.; Brandtzaeg, P. *Lancet* **2007**, *369*, 2196-2210.

(9) Vann, W. F.; Tavarez, J. J.; Crowley, J.; Vimr, E.; Silver, R. P. *Glycobiology* **1997**, *7*, 697-701.

(10) Robbins, J. B.; McCracken, G. H., Jr.; Gotschlich, E. C.; Orskov, F.; Orskov, I.; Hanson, L. A. *N. Engl. J. Med.* **1974**, *290*, 1216-20.

(11) Smith, H.; Parsons, N. J.; Cole, J. A. *Microb. Pathog.* **1995**, *19*, 365-77.

(12) Stein, D. M.; Robbins, J.; Miller, M. A.; Lin, F. Y.; Schneerson, R. *Vaccine* **2006**, *24*, 221-8.

(13) Bagnoli, F.; Rappuoli, R. *Drug Discov. Today. Dis. Mech.* **2006**, *3*, 273-279.

(14) Rees, J. H.; Soudain, S. E.; Gregson, N. A.; Hughes, R. A. *N. Engl. J. Med.* **1995**, *333*, 1374-9.

(15) Moran, A. P.; Prendergast, M. M. *J. Autoimmun.* **2001**, *16*, 241-56.

(16) Tanner, M. E. *Bioorg. Chem.* **2005**, *33*, 216-228.

(17) Ray, P. H. *J. Bacteriol.* **1980**, *141*, 635-44.

(18) Asojo, O.; Friedman, J.; Adir, N.; Belakhov, V.; Shoham, Y.; Baasov, T. *Biochemistry* **2001**, *40*, 6326-6334.

(19) Bentley, R. *Crit. Rev. Biochem. Mol. Biol.* **1990**, *25*, 307-84.

(20) Hao, J.; Balagurumoorthy, P.; Sarilla, S.; Sundaramoorthy, M. *Biochem. Biophys. Res. Commun.* **2005**, *338*, 1507-14.

(21) Gunawan, J.; Simard, D.; Gilbert, M.; Lovering, A. L.; Wakarchuk, W. W.; Tanner, M. E.; Strynadka, N. C. *J. Biol. Chem.* **2005**, *280*, 3555-63.

(22) Hedstrom, L.; Abeles, R. *Biochem. Biophys. Res. Commun.* **1988**, *157*, 816-20.

(23) DeLeo, A. B.; Sprinson, D. B. *Biochem. Biophys. Res. Commun.* **1968**, *32*, 873-7.

(24) Li, Z. L.; Sau, A. K.; Shen, S. D.; Whitehouse, C.; Baasov, T.; Anderson, K. S. *J. Am. Chem. Soc.* **2003**, *125*, 9938-9939.

(25) Clark, M. E.; Berti, P. J. *Biochemistry* **2007**, *46*, 1933-40.

(26) Liu, F.; Lee, H. J.; Strynadka, N. C. J.; Tanner, M. E. *Biochemistry* **2009**, *48*, 9194-9201.

(27) Tovar-Mendez, A.; Rodriguez-Sotres, R.; Lopez-Valentin, D. M.; Munoz-Clares, R. A. *Biochem. J.* **1998**, *332 (Pt 3)*, 633-42.

(28) Tovar-Mendez, A.; Munoz-Clares, R. A. *Biochim. Biophys. Acta.* **2001**, *1546*, 242-52.

(29) Sundaram, A. K.; Pitts, L.; Muhammad, K.; Wu, J.; Betenbaugh, M.; Woodard, R. W.; Vann, W. F. *Biochem. J.* **2004**, *383*, 83-9.

(30) Furdui, C. M.; Sau, A. K.; Yaniv, O.; Belakhov, V.; Woodard, R. W.; Baasov, T.; Anderson, K. S. *Biochemistry* **2005**, *44*, 7326-35.

(31) Radaev, S.; Dastidar, P.; Patel, M.; Woodard, R. W.; Gatti, D. L. *J. Biol. Chem.* **2000**, *275*, 9476-84.

(32) Shumilin, I. A.; Kretsinger, R. H.; Bauerle, R. H. *Structure* **1999**, *7*, 865-75.

(33) Voet, D.; Voet, J. G. *Biochemistry*; 3 ed.; Wiley, 2004.

(34) Segal, I. R. *Enzyme Kinetics: Behavior and Analysis of Rapid Equilibrium and Steady-State Enzyme Systems*; Wiley, 1975.

(35) Silverman, R. B. *The Organic Chemistry of Enzyme-Catalyzed Reactions*; Revised ed.; Academic Press, 2002.

(36) Schramm, V. L. *Annu Rev Biochem* **1998**, *67*, 693-720.

(37) Cox, N. *Lehninger Principles of Biochemistry*; 3 ed.; W.H. Freeman, 2000.

(38) Wolfenden, R.; Snider, M. J. *Accounts Chem. Res.* **2001**, *34*, 938-945.

(39) Berti, P. J.; McCann, J. A. B. *Chem. Rev.* **2006**, *106*, 506-555.

(40) Morrison, J. F.; Walsh, C. T. *Adv. Enzymol. Relat. Areas Mol. Biol.* **1988**, *61*, 201-301.

(41) Morrison, J. F. *Trends Biochem. Sci.* **1982**, *7*, 102-105.

(42) Waley, S. G. *Biochem. J.* **1993**, *294*, 195-200.

(43) Du, S.; Faiger, H.; Belakhov, V.; Baasov, T. *Bioorg. Med. Chem.* **1999**, *7*, 2671-82.

(44) Grison, C.; Petek, S.; Finance, C.; Coutrot, P. *Carbohydr. Res.* **2005**, *340*, 529-37.

(45) Belakhov, V.; Dovgolevsky, E.; Rabkin, E.; Shulami, S.; Shoham, Y.; Baasov, T. *Carbohydr. Res.* **2004**, *339*, 385-392.

(46) Walker, S. R.; Parker, E. J. *Bioorg. Med. Chem. Lett.* **2006**, *16*, 2951-2954.

(47) Morrison, E., MSc Thesis, McMaster University, NeuNAc oxime: A New Inhibitor for Sialic Acid Synthase, 2009.

(48) Lanzetta, P. A.; Alvarez, L. J.; Reinach, P. S.; Candia, O. A. *Anal. Biochem.* **1979**, *100*, 95-97.

(49) Jakeman, D. L.; Evans, J. N. S. *Bioorg. Chem.* **1998**, *26*, 245-253.

(50) Blacklow, R. S.; Warren, L. *J. Biol. Chem.* **1962**, *237*, 3520-6.

(51) Stephens, C. M.; Bauerle, R. *J. Biol. Chem.* **1991**, *266*, 20810-7.

(52) Kohen, A.; Jakob, A.; Baasov, T. *Eur. J. Biochem.* **1992**, *208*, 443-9.

(53) DeLeo, A. B.; Sprinson, D. B. *J. Bacteriol.* **1975**, *124*, 1312-20.

(54) Sullivan, T. J.; Truglio, J. J.; Boyne, M. E.; Novichenok, P.; Zhang, X.; Stratton, C. F.; Li, H. J.; Kaur, T.; Amin, A.; Johnson, F.; Slayden, R. A.; Kisker, C.; Tonge, P. J. *ACS Chem. Biol.* **2006**, *1*, 43-53.

(55) Pargellis, C.; Tong, L.; Churchill, L.; Cirillo, P. F.; Gilmore, T.; Graham, A. G.; Grob, P. M.; Hickey, E. R.; Moss, N.; Pav, S.; Regan, J. *Nat. Struct. Biol.* **2002**, *9*, 268-72.

(56) Jackson, S. G.; Zhang, F.; Chindemi, P.; Junop, M. S.; Berti, P. J. *Biochemistry* **2009**, *48*, 11715-23.

(57) Totoritis, R.; Duraiswami, C.; Taylor, A. N.; Kerrigan, J. J.; Campobasso, N.; Smith, K. J.; Ward, P.; King, B. W.; Murrayz-Thompson, M.; Jones, A. D.; Van Aller, G. S.; Aubart, K. M.; Zalacain, M.; Thrall, S. H.; Meek, T. D.; Schwartz, B. *Biochemistry* **2011**, *50*, 6642-54.

(58) Eftink, M. R.; Anusiem, A. C.; Biltonen, R. L. *Biochemistry* **1983**, *22*, 3884-96.

(59) Copeland, R. A. *Methods Biochem. Anal.* **2005**, *46*, 1-265.

(60) Dadi, P. K.; Ahmad, M.; Ahmad, Z. *Int. J. Biol. Macromol.* **2009**, *45*, 72-9.

(61) Callan, O. H.; So, O. Y.; Swinney, D. C. *J Biol Chem* **1996**, *271*, 3548-3554.

(62) Kulmacz, R. J.; Lands, W. E. M. *J Biol Chem* **1985**, *260*, 2572-2578.

(63) Ouellet, M.; Percival, M. D. *Biochem. J.* **1995**, *306*, 247-251.

(64) Johnson, A. R.; Marletta, M. A.; Dyer, R. D. *Biochemistry* **2001**, *40*, 7736-45.

(65) Taraska, J. W.; Puljung, M. C.; Olivier, N. B.; Flynn, G. E.; Zagotta, W. N. *Nat. Methods* **2009**, *6*, 532-7.

(66) Taraska, J. W.; Puljung, M. C.; Zagotta, W. N. *Proc. Natl. Acad. Sci. U.S.A.* **2009**, *106*, 16227-32.